▌**Photochemistry**
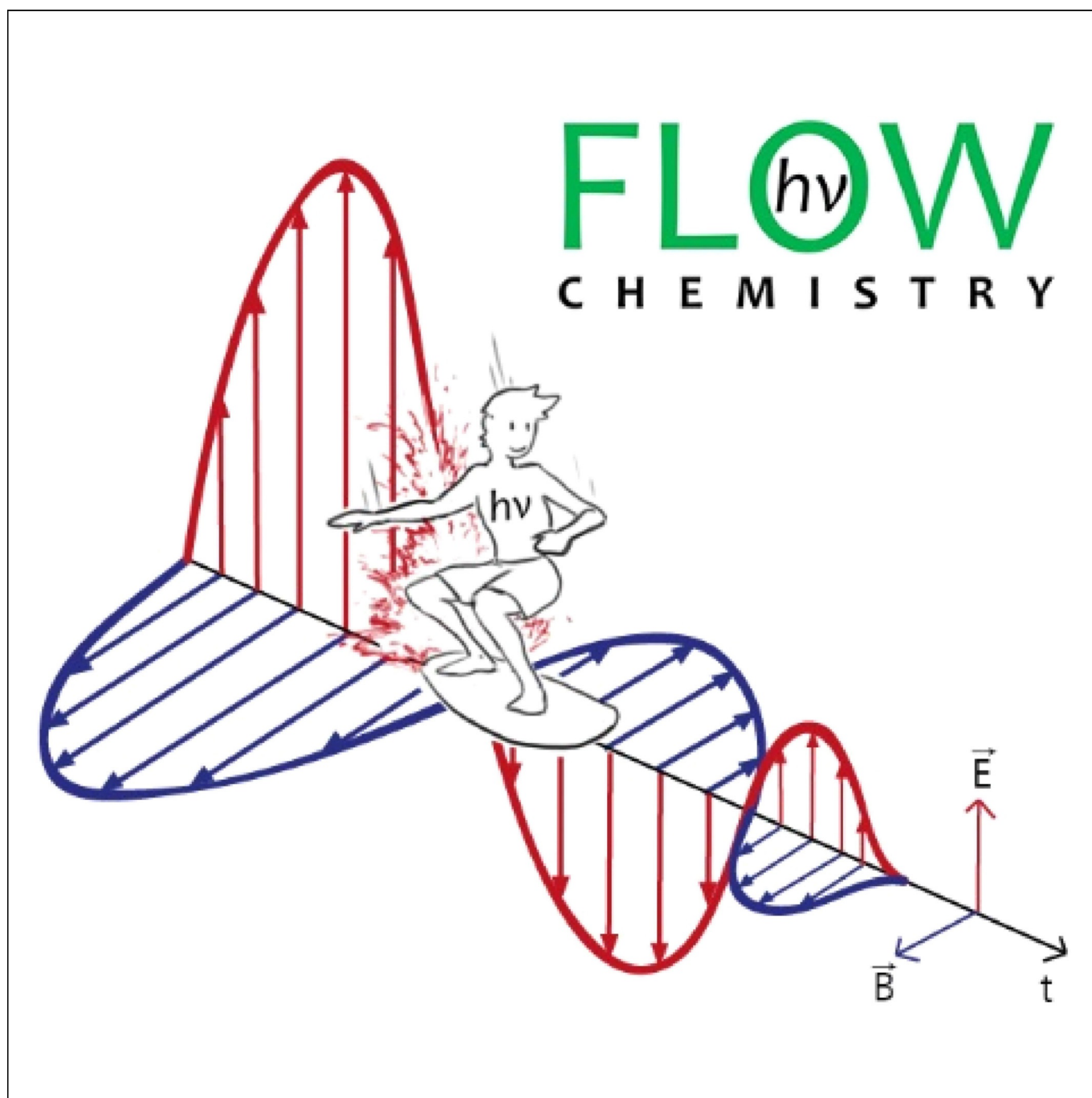
Flow Photochemistry as a Tool in Organic Synthesis

Thomas H. Rehm*[a]

Dedicated to Professor Siegfried Hünig on the occasion of his 99th birthday

Abstract: Photochemical transformations of molecular building blocks have become an important and widely recognized research field in the past decade. Detailed and deep understanding of novel photochemical catalysts and reaction concepts with visible light as the energy source has enabled a broad application portfolio for synthetic organic chemistry. In parallel, continuous-flow chemistry and microreaction technology have become the basis for thinking and doing chemistry in a novel fashion with clear focus on improved process control for higher conversion and selectivity.

As can be seen by the large number of scientific publications on flow photochemistry in the recent past, both research topics have found each other as exceptionally well-suited counterparts with high synergy by combining chemistry and technology. This review will give an overview on selected reaction classes, which represent important photochemical transformations in synthetic organic chemistry, and which benefit from mild and defined process conditions by the transfer from batch to continuous-flow mode.

1. Introduction

1.1 Benefits of performing synthesis in continuous flow

The goal for continuous-flow chemistry is to overcome the challenges and problems of classical synthesis concepts in batch vessels, for example, less efficient process control, moderate conversion and selectivity, high energy consumption, and long reaction times.[1] In general, the overall concept of continuous-flow chemistry can be described as a technological environment that allows continuous mixing and reacting of physical phases in a small and defined volume under highly controlled conditions.[2] This theoretical definition gives an outlook on several advantages for running synthesis in continuous-flow mode:

1) A small reaction volume, encased in a solid and robust reactor housing, can be used for high-pressure and high-temperature reactions with the advantage of quick and efficient heating and cooling for nearly perfect process control and higher conversion.

2) Mixing of substrates with reagents or quenching of reaction solutions can be done far more efficient on a small volume scale with the advantage of higher selectivity (less byproducts).

3) The flow rates of the substrate and reagent solutions determine the residence time inside the reactor with the advantage of exact time control of phase contacting under defined physical conditions.

4) Heterogeneous catalysts can be immobilized inside the small reactor volume with the advantage of less complicated workup and product separation.

5) In the case of photochemical reactions, small reaction volumes like thin films in open microchannels or fine streams in capillaries can be fully irradiated during the residence time in the reactor with the advantage of higher conversion and selectivity owing to less over-irradiation and consecutive degradation.[3]

6) Modern LED technology allows the construction of very small and adaptable light sources for flow photoreactors with the advantage of less energy consumption and less safety issues and heat management compared with standard mercury or xenon lamps.[4] Based on the aforementioned advantages, flow photochemistry has also come into the focus for detailed investigations by chemical engineers. Hence, a deeper and more detailed understanding of the physical and engineering challenges and pitfalls is available now through the characterization of photoreactor equipment and concepts.[5] This knowledge is most beneficial for chemists, as it helps to understand why some reactions work properly, but some of them do not yield the expected results.[5, 6]

Nevertheless, continuous-flow photochemistry has become an accepted research field as well owing to the fact that simple flow reactors can be built from inexpensive materials (e.g., polymer capillaries, LEDs), whereas in parallel many companies provide modular concepts for continuous-flow synthesis including high-power light sources for photochemistry.[7, 8] These technological prerequisites to improve light–matter interactions on a smaller length scale have lowered the gap for doing chemistry with technology and resulted in countless publications from research groups worldwide that have transferred their expertise in photochemistry from batch to flow mode.[9–12]

1.2 Progress in visible light photochemistry and photocatalysis

Besides the technological achievements mentioned above, the field of photochemistry applied to organic synthesis was revitalized in the last decade as well. The key reason for this rapid

[a] Dr. T. H. Rehm
Division Energy & Chemical Technology/Flow Chemistry Group
Fraunhofer Institute for Microengineering and Microsystems IMM
Carl-Zeiss-Straße 18–20, 55129 Mainz (Germany)
E-mail: thomas.rehm@imm.fraunhofer.de
Homepage: https://www.imm.fraunhofer.de
https://www.flowphotochemistry.com

The ORCID identification number(s) for the author(s) of this article can be found under: https://doi.org/10.1002/chem.202000381.

Chemistry–A European Journal

Review
doi.org/10.1002/chem.202000381

Chemistry Europe
European Chemical
Societies Publishing

development can be attributed to the application of visible light as an energy carrier. Spatially and energetically defined irradiation with visible light allows mild and selective activation of photocatalysts or substrate–catalyst complexes.[13] Well-known, but expensive ruthenium or iridium metal complexes have been used widely, however, they have to compete with less expensive copper, iron, or chromium centered metalorganic complexes.[13e,p,14] In addition, the use of metal-free sensitizers like biological-derived catalysts of Rose Bengal, porphyrin, or riboflavin derivatives broadens the application range of photocatalysis with visible light as well.[13g,15] In particular, the development of tailor-made high-performance dyes and layered materials like perylene diimides or graphitic carbon nitride plays a major role for these purely organic photocatalytically active materials.[16,17] In addition, various charts are available in reviews or other formats that summarize photocatalytically active compounds and provide a very good overview on their use in photooxidation or -reduction.[13g,j,18] On the other hand, inorganic semiconductor materials contribute as well to the application of photochemistry in fine chemicals synthesis. Besides TiO_2, as the most prominent semiconductor, bismuth and tungsten oxides have been used as selective photocatalysts in batch and flow.[13b,19] Organic–inorganic hybrid materials or specifically doped semiconductors were developed to shift the absorption range of the pure materials towards the region of visible light.[13b,20] In recent years, so-called dual catalysis concepts have been recognized as well for photochemical transformations in conjunction with other classical catalyst systems for, for example, light-triggered activation with subsequent metal catalyst-based conversion.[21] Stereoselective conversion of substrates became available by merging organocatalysis with photochemistry. Activation of the substrate by chiral additives like amino acid-based organocatalysts and photochemical conversion with either an organometallic complex or as colored electron donor–acceptor (EDA) complexes represents an elegant way to introduce chiral centers into substrates. In particular, the in situ formation of EDA complexes is of high interest. The single compounds of the complex usually have no absorption in the visible light, but upon complexation charge transfer can occur, which results in a new absorption band with $\lambda_{max} > 400$ nm. In consequence, such supramolecular substrate assemblies do not necessarily need a separate photocatalyst for the desired molecular transformation.[22] On the contrary, less reactive substrates with strong bonds between, for example, aryl carbon and halogen atoms can be converted with special photocatalysts that allow a consecutive excitation. This concept is based on the two-fold light absorption in separate steps. The first absorption results in a stable photocatalyst intermediate (e.g., radical anion), which then can absorb a second photon to reach the excited state with high reduction potential. Aryl chlorides could be cleaved by this pathway and used for C–C bond formation without expensive noble metal catalysts.[16a,b,23] All these enticing results stimulated the whole field of photocatalyst development with the aims of specific light absorption properties and reduction or oxidation potentials as well as the deep understanding of photophysical processes from catalyst excitation to interaction with the substrate

and final conversion to the product.[24] This summarizing introduction demonstrates the vitality of photochemistry and application-related research looking for novel synthesis routes under mild and selective conditions as alternative to classic thermal chemistry.

1.3 Scope of this review

The beneficial use of microreaction technology and continuous-flow concepts for improving photochemical synthesis routes has been discussed and published in several reviews and books.[3–9,25] Based on this literature, one can assume that another review on this topic is not necessary anymore. But photocatalysis is a highly vivid and productive research field, especially in conjunction with flow technology. The number of publications on this research field increase nearly on a weekly basis (Figure 1). But as usual, a review cannot cover all examples on a specific topic, but needs a selection of interesting examples from the large number of available publications. Hence, a decision was made for examples that represent im-
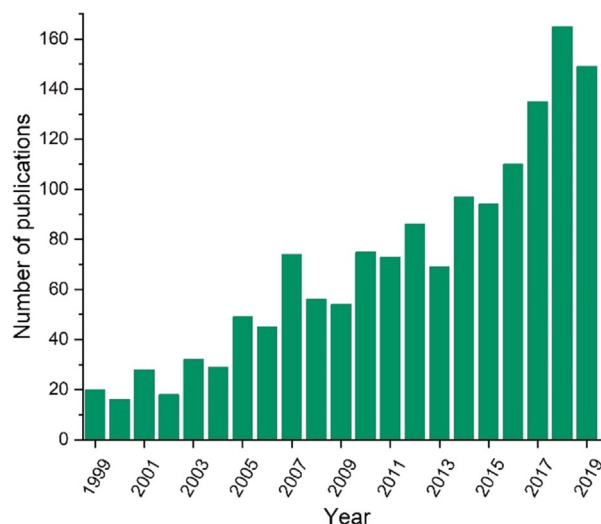
Figure 1. Number of publications per year from 1999 to 2019 for the topics "photocatalysis" AND "flow" derived from Web of Science database analysis.[26]

Thomas Rehm studied chemistry at the Julius Maximilians University in Würzburg, Germany, and finished his Ph.D. thesis in 2008 with Carsten Schmuck, focusing on supramolecular polymer chemistry in polar solutions. Afterwards, he joined the group of Frank Würthner at the same university and worked on perylene diimides for DNA/RNA recognition. In 2011, he started a new position at Fraunhofer IMM in Mainz, Germany, working on continuous-flow chemistry. His research is focused on the use of microreaction technology for photochemical applications in flow.

portant chemical transformations such as, for example, oxygenations, C–X coupling reactions, and incorporation of various functional groups or defined changes in the molecular substrate structure. Some examples will also be presented that are part of a reaction sequence with reactive intermediates. In this case, continuous-flow chemistry is excellently suited for the in situ generation of such compounds with immediate use in the next step. In summary, eleven reaction classes have been selected. Up to three examples will be presented per reaction class and discussed according to the specific advantages of continuous-flow photoreactor equipment, for example, increased safety, lower energy consumption, or better conversion and selectivity by improved mixing and advanced process control. Throughout the manuscript yields are given for the flow reactions. If possible, these values will be compared with the results from the batch reactions. Finally, the review ends with a conclusion and an outlook on future trends for this vibrant research field.

## 2. Recent Synthesis Concepts with Flow Photochemistry

2.1 Photooxygenation with $^1O_2$

The photochemical in situ formation of singlet oxygen has gained great importance for the mild synthesis of natural products and drugs such as artemisinin **4**, one of the most important ingredients for anti-malaria drugs (Figure 2).[27] In 2012, the Seeberger group developed the continuous-flow synthesis of this active pharmaceutical ingredient (API)-based on a fluorinated ethylene propylene (FEP) capillary reactor, which was used to contact the liquid phase with oxygen gas in slug flow. Here, flow reactor equipment with small reaction volumes is particularly useful for the safe handling of pure oxygen gas and its transformation into singlet oxygen for synthetic applications. Primarily, *meso*-tetraphenylporphyrin (TPP) or 9,10-di-
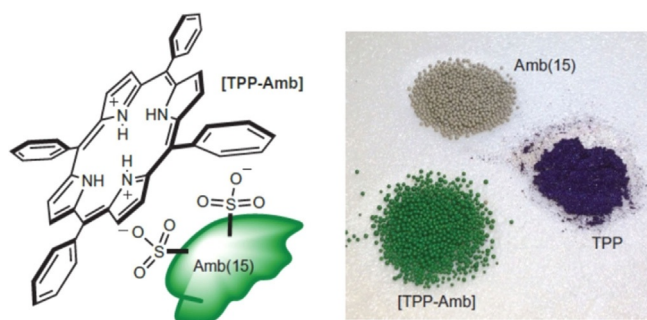
cyanoanthracene (DCA) were used as a sensitizer with a medium-pressure Hg lamp or LEDs as light source.[28]

Meanwhile, this process was re-invented by the same group by utilizing the crude toluene extract of *Artemisia annua* leaves as a natural source.[29] Besides the starting material dihydroartemisinic acid **1**, the extract also contains natural chlorophylls, which were applied as sensitizers for the singlet oxygen formation. The strong light absorption of the extract at 416 and 672 nm by the natural sensitizers allows the adaptation of the LED arrays of the flow reactor setup to 420 and 660 nm. For comparison of the novel process to already published results, the crude extract was enriched with pure **1** to a concentration of 0.5 M. Trifluoroacetic acid (TFA) was also added to the extract (0.375 M) to enable the acid-catalyzed Hock cleavage in the second step of the flow synthesis (see Figure 2). The flow photoreactor (FEP, 5 mL) was set to a temperature of −20 °C and irradiated either with 420 or 660 nm. In the case of 420 nm LED emission wavelength, a yield of 88% was obtained for the hydroperoxide intermediate after 5 min, whereas irradiating the reaction solution with 660 nm resulted in approximately the same yield of 87% after only 3 min. Subsequent transformation of the hydroperoxide intermediate **2** through the Hock cleavage and oxidation in a second capillary reactor (FEP, 7 bar, 30 °C, $\tau_{res} = 10$ min) gave the desired product artemisinin **4** in 64% yield, which is slightly lower than the flow synthesis with 69% when using pure substrates and catalysts. Of course, the crystallization of the artemisinin might become more complicated from the extract solution than from the cleaner full synthetic solution, but this work clearly shows the potential of chlorophylls as natural and easy to apply sensitizers.

The work of Seeberger et al. can be regarded as a starting point for several other projects related to the synthesis route and synthesis process of **4**. For example, Kappe et al. presented a flow reduction of artemisinic acid to dihydroartemisinic acid **1** by in situ generated diimide from hydrazine.[30] Feth et al. optimized the photochemical oxidation step in the industrial synthesis of **4** by using process analytical tools like ATR-MID-IR (attenuated total reflection middle infrared) and UV/Vis spectroscopy to monitor the reaction kinetics.[27a] Noël et al. used a novel flow reactor concept based on luminescent light concentrator technology for the synthesis of **4** with solar light.[31] Amara et al. turned their focus to the optimization of the environmental aspects of artemisinin synthesis.[32] They developed a catalyst system that allowed a dual-use of sulfonated cross-linked polystyrene as a Brønsted acid (instead of TFA for the Hock cleavage) and as the heterogeneous support for TPP as the sensitizer. The di-protonation of the porphyrin core leads to non-covalent ionic interactions between the sensitizer and the ion-exchange resin (Figure 3). This concept allows a straightforward immobilization of TPP on the surface of the polystyrene beads with negligible leaching of TPP. The strategy of George et al. also envisages the use of liquid carbon dioxide as the main solvent and oxygen gas carrier at a low temperature of 5 °C. A flow photoreactor setup was designed with a sapphire glass tube as the main element and three LED arrays as a daylight source. Liquid CO_2 was transferred from a reser-
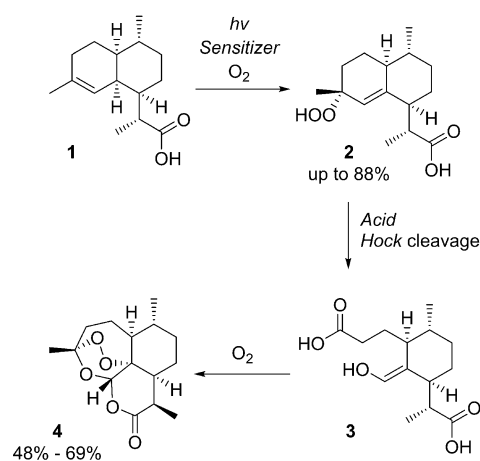
Figure 2. Three-step synthesis of artemisinin **1** with air as the oxygen source: photooxygenation with $^1O_2$; acid-catalyzed Hock cleavage and rearrangement; oxidation with $^3O_2$ (other hydroperoxides and tautomers are omitted for clarity).

Chemistry–A European Journal

Review
doi.org/10.1002/chem.202000381

**Chemistry
Europe**

European Chemical
Societies Publishing

Figure 3. Heterogenized sensitizer on acidic polymer support for the continuous-flow synthesis of artemisinin in liquid CO_2. Reproduced with permission from ref. [32], copyright 2015 Springer Nature.

Figure 4. Top: Cyanation of benzylamine **5** via imine intermediate **6** trapped by cyanide at low temperature ($\tau_{res} = 3$ min; TPP = *meso*-tetraphenylporphyrin, TMSCN = trimethylsilyl cyanide, TBAF = tetrabutylammonium fluoride). Bottom: Neopentylamine **8** as the starting material for the synthesis of D,L-*tert*-leucine hydrochloride **9**.

voir with a cooled HPLC pump to a static stainless-steel mixer, where it was contacted with oxygen gas for a final concentration of 2 mol%. Starting material **1** was fed as a toluene solution (0.1 M) with a HPLC pump into a second static mixer, where it was mixed with the liquid CO_2/O_2 stream. The system pressure was set to 180 bar and the mixed substrate streams were transferred into the sapphire glass photoreactor containing the dual-function catalyst.

Within four passes, 98% conversion could be achieved with a yield of 51% for **4**. This process was then optimized with a photoreactor of doubled length and residence time, yielding approximately full conversion with a slightly decreased yield of 48% in one pass. George et al. could show several advantages with this flow approach: a) the acidic environment of the heterogeneous catalyst support pushes the reaction selectively to the Hock cleavage as already seen in homogeneous batch reactions,[33] and b) a second step with prolonged heating and an oxygen atmosphere is no longer necessary, which is in contrast to the synthesis developed by Seeberger et al.[28] In addition, the use of chlorinated solvents like CH_2Cl_2 or relatively toxic TFA is no longer needed. The immobilization of the sensitizer also allows an easier crystallization of artemisinin **4** with greatly minimized contamination with TPP.

2.2 Cyanation

The incorporation of cyanide groups into molecules allows the construction of nitrogen-containing compounds with great versatility for subsequent derivatization to, for example, amines, amides, or carboxylic acids.[34] At room temperature the oxidative addition of cyanides to primary amines mostly results in dimeric products. Seeberger et al. circumvented this problem by running the oxidative Strecker reaction at $-50\,°C$ with singlet oxygen as the primary oxidant for the formation of the imine intermediate (Figure 4).[35] Efficient gas–liquid contacting was made possible as slug flow in a capillary reactor (FEP, 7.5 mL, $\tau_{res} = 3$ min) at 8 bar system pressure. Singlet oxygen was formed in situ by using TPP as the sensitizer and an LED array as a light source with an emission wavelength at 420 nm, perfectly fitting to the Soret absorption band of the porphyrin core. With this setup it was possible to oxidize activated (benzylic) and unactivated amines to the corresponding
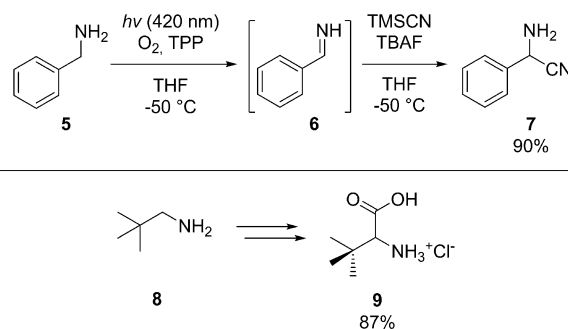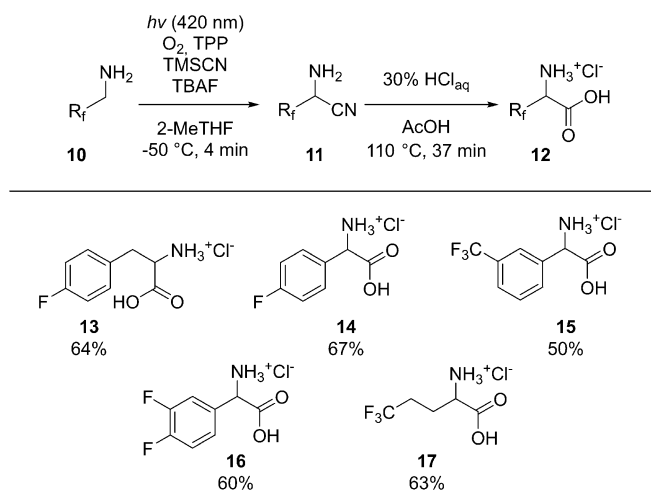
imines, which were then converted to α-amino nitriles with trimethylsilyl cyanide (TMSCN) as the cyanide source and tetrabutylammonium fluoride (TBAF) for activation of the silyl group. In the case of benzylamine (**5**), a yield of 90% was possible. As an example for subsequent derivatization of the cyanide group, neopentylamine **8** was first converted to its α-amino nitrile and then hydrolyzed to D,L-*tert*-leucine hydrochloride **9** in 87% yield over both steps (Figure 4).

The same strategy was also used for the flow synthesis of fluorinated α-amino acids. Seeberger et al. developed a semicontinuous two-step synthesis, which in the first step converts primary amines with fluorinated side chains (**10**) to the respective amino nitriles **11** by using the above-described photoreactor setup and process ($-50\,°C$, 7 bar, $\tau_{res} = 4$ min).[36] After solvent exchange from 2-MeTHF (2-methyl tetrahydrofuran) to acetic acid and aqueous HCl, **11** was hydrolyzed in a second capillary reactor (22 mL, $\tau_{res} = 37$ min) at $110\,°C$ and 8 bar to the corresponding amino acid **12** (Figure 5). Fluorinated homobenzylic and benzylic amines were converted to fluorinated amino acids **13** and **14**–**17** with moderate yields between 50 and 67%. The quick and straightforward use of the crude intermediate mixture from the first synthesis step in a flow reactor also allowed the conversion of the 4,4,4-trifluorobutylamine to **17** in 64% yield although its alkyl amino nitrile tends to decompose upon purification.

Contrary to the above-mentioned examples, Opatz et al. used sunlight instead of artificial irradiation from LED arrays.[37] A FEP capillary (25 m, approx. 20 mL) was braided and stabilized along a wire netting, which also prevented self-shadowing of the capillary. The reactor was directly oriented to the sun and repositioned every hour for maximum solar radiation on sunny and non-hazy days between May and August in Mainz, Germany. With this setup, several substrates were screened for the oxidative cyanation of tertiary amines. Rose Bengal was used as the sensitizer for the in situ formation of singlet oxygen in slug flow and KCN was the cyanide source. Their "sunflow" approach outperformed the batch reaction in time and yield. In the case of isoquinoline **18**, the flow synthesis yielded the product **19** in 93% within 5 min, whereas the batch synthesis reached only 80% yield in 180 min (Figure 6).

Chemistry–A European Journal

Review
doi.org/10.1002/chem.202000381

Chemistry Europe
European Chemical
Societies Publishing

Figure 5. Top: Semi-continuous synthesis of fluorinated α-amino acids by ox-idative cyanation of fluorine-containing primary amines (TPP = *meso*-tetra-phenylporphyrin, TMSCN = trimethylsilylcyanide, TBAF = tetrabutylammoni-um fluoride). Bottom: Examples of fluorinated amino acids obtained with the two-step cyanation/hydrolization of amines.
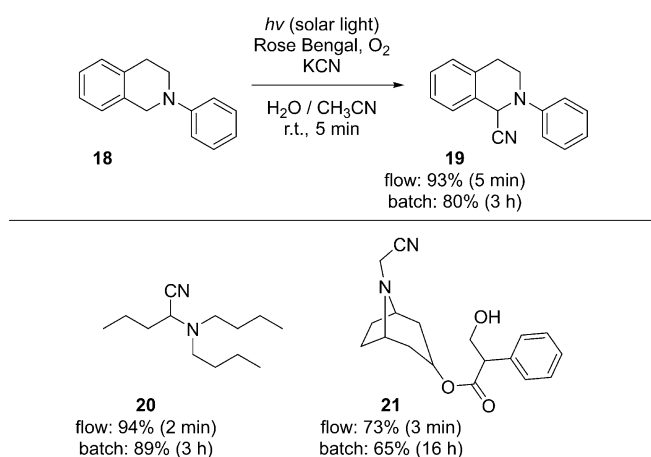
Figure 6. Top: Strongly accelerated cyanation of tertiary amines by the use the "sunflow" capillary photoreactor. Bottom: Simple (**20**) and complex amines (**21**) can be easily converted to their cyanated derivatives.

Even more impressive is the performance for a simple alkyl amine like tributylamine. Within 2 min 94 % yield for **20** was reached compared with 89 % in 180 min for the batch synthe-sis. Atropine, a more complex and biological relevant tertiary amine, was converted to **21** with 73 % yield in 3 min. Here, the batch synthesis was far behind with 65 % yield in 960 min. These examples clearly show that photochemistry can be per-formed in a more sustainable way by resorting to massively available energy resources like solar radiation.

2.3 Hydrogen atom transfer (HAT) reactions

Hydrogen atom transfer reactions are considered as an excel-lent tool for the selective activation of R–H bonds with subse-quent formation of new bonds to carbon atoms or hetero-atoms.[38] In particular, the use of catalysts with decatungstate

anions $[W_{10}O_{32}]^{4-}$ as the photoactive material allows the mild activation of C–H bonds to radicals with subsequent addition to, for example, electron-deficient olefins.[39] This reaction path-way was described by Protti et al. for the two-step flow synthe-sis of γ-lactones from aldehydes and α,β-unsaturated esters.[40] Heptanal **22** and diethylmaleate **23** (each 0.2 M in acetonitrile) were chosen as model substrates for the process development in a capillary photoreactor (polytetrafluoroethylene (PTFE), 12 mL) and with a medium-pressure Hg lamp (125 W) as the light source. Tetrabutylammonium decatungstate (TBADT) was applied as the photocatalyst (2 mol %) for the in situ formation of the acyl radical from heptanal. Within a residence time of $\tau_{res} = 120$ min (corresponding to a flow rate $f_l = 0.1$ mL min^{-1}), the desired acyl succinate **24** was obtained in 67 % yield against 44 % within 24 h in batch mode. The product stream containing **24** was then mixed in a T-piece with a solution of NaBH$_4$ (0.4 M in EtOH, $f_l = 0.1$ mL min^{-1}) and fed into a second capillary reactor (10 mL, $\tau_{res} = 50$ min). The ketone was efficient-ly reduced, yielding the γ-hydroxy ester, which cyclized to the desired γ-lactone **25** upon acidic workup in 65 % overall yield (Figure 7). With this flow approach the photocatalyzed step was done in only 120 min compared with the 24 h necessary in batch mode. Finally, the space time yield of the flow photo-reactor is 67 mmol L^{-1} h^{-1}, which is approximately six times higher than the batch synthesis.

In a second example, decatungstate was used for the very important oxyfunctionalization of aliphatic amines in the β- and γ-positions via HAT as the key step.[41] Usually, free aliphat-ic amines are only hydroxylized at the nitrogen atom or in the C$_\alpha$-position. Schultz et al. deactivated this directing functionali-ty of the amine nitrogen atom by protonation. This step en-ables the selective conversion of remote and less-activated methylene groups in the β- and γ-positions to ketones by HAT reactions with decatungstate as the photocatalyst. After high-throughput screening of the reaction conditions in batch mode, the model substrate pyrrolidine **26** (0.7 M in aqueous acetonitrile solution) was converted after 2 h of irradiation with UV light at 365 nm to pyrrolidin-3-on **27** in 65 % yield. Op-timal reaction conditions were found to be 1 mol % sodium decatungstate (NaDT), 1.5 equivalents H$_2$SO$_4$ for protonation, and 2.5 equivalents H$_2$O$_2$ as oxidant. The exclusion of acid led
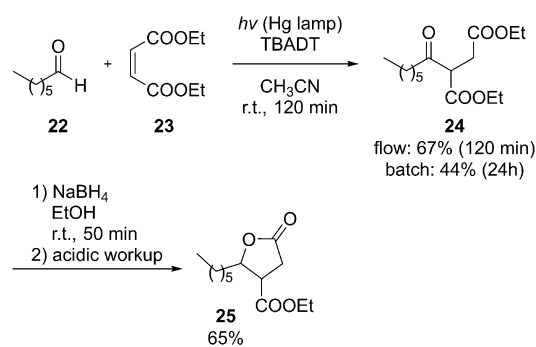
Figure 7. Two-step flow synthesis of γ-lactones by decatungstate photocata-lyzed HAT reaction in the first step (TBADT = tetrabutylammonium decatung-state).

solely to the formation of *N*-hydroxypyrrolidine. Omission of light or photocatalyst only results in traces of the desired product. The reaction fails as well with visible light (420 or 450 nm) instead of UV light, which supports the assumption that decatungstate is the photoactive catalyst for the HAT reaction. Schultz et al. were able to functionalize several primary linear and secondary cyclic amines as well as amino acids with ketone groups in remote positions. The authors used flow reactor equipment for scaling-up the oxygenation of pyrrolidine **26** to 5 g (Figure 8). Instead of H_2O_2, oxygen gas was used as the terminal oxidant ($f_l = 0.5$ mL min^{-1}) and mixed with the substrate solution ($f_l = 1$ mL min^{-1}) in a T-piece prior to the inlet of the capillary photoreactor (FEP, 10 mL). An LED array was used as the light source with a main emission wavelength at 365 nm (16 W radiant power). The system pressure was set to 4.5–5 bar for stable gas–liquid contacting in slug flow. After circulating the reaction solution for 22 h, pyrrolidin-3-on **27** was obtained in 56% yield corresponding to a space time yield of 15 mmol h^{-1} mL^{-1}.
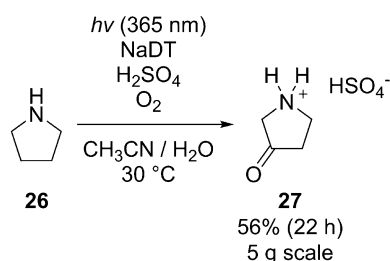
Figure 8. Oxyfunctionalization of pyrrolidine **26** with HAT in the remote and less-activated C$_\beta$ position (NaDT = sodium decatungstate).

The photocatalytic oxidation of activated and unactivated methylene groups in cyclic and linear alkanes was investigated under flow conditions by Noël et al.[42] Process development was done with cyclohexane **28** as the model substrate (143 mM), pure oxygen gas as the oxidant, and tetrabutylammonium decatungstate (TBADT) as the photocatalyst in acetonitrile acidified with aqueous hydrochloric acid (1 M, 2.5:1). The reaction screening was performed in a capillary photoreactor (perfluoroalkoxy (PFA), 5 mL) at room temperature using an LED array with 365 nm emission wavelength. With 5 mol% TBADT at normal pressure with a residence time of $\tau_{res} = 45$ min, the conversion of **28** yielded 81% cyclohexanone **29** and 9% cyclohexanol **30** (Figure 9). Compared with the synthesis in batch mode, the flow synthesis was faster by a factor of 18 (13 min vs. 4 h at 53% yield with 2 mol% TBADT). The faster conversion can be attributed to the increased oxygen gas mass transfer in slug flow and improved light penetration through the thin films and the liquid slugs.

Based on these optimized reaction conditions, a broad scope of activated methylene groups in benzylic or allylic positions were oxidized to ketones; for example, cyclohexene to cyclohexen-1-one **31** (70%) or 1,3-dihydro-2-benzofuran to 2-benzofuran-1-one **32** (71%). Unactivated methylene groups were also converted very efficiently, as in the cases of cyclo-
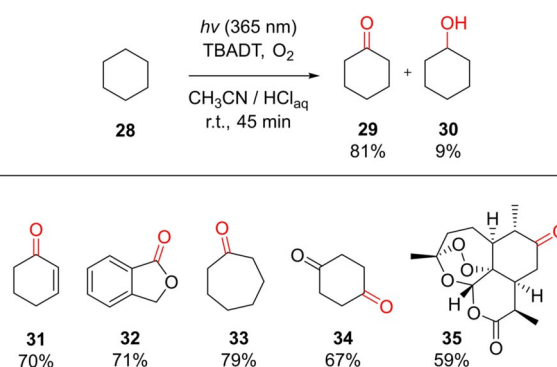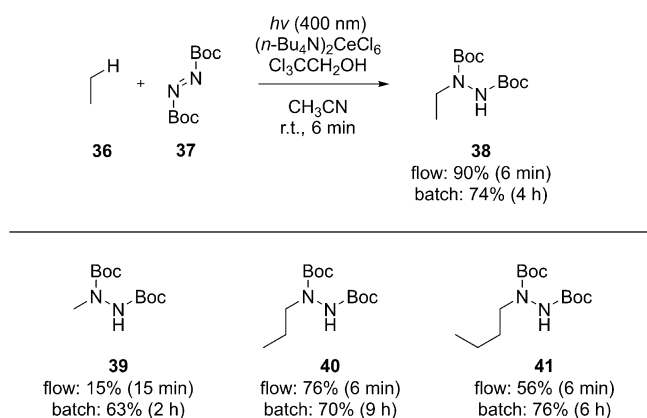
Figure 9. Top: Decatungstate-based C(sp^3)–H aerobic oxidation of cyclohexane (TBADT = tetrabutylammonium decatungstate). Bottom: Activated and unactivated C–H bonds oxidized with decatungstate anions as the HAT photocatalyst.

heptane to cycloheptanone **33** (79%) and cyclohexanone to cyclohexan-1,4-dione **34** (67%). Even very complex structures like artemisinin **4** were oxidized to artemisitone-9 **35** on the 5 mmol scale in 59% yield. The work of Noël et al. is a very good example of the safe and straightforward use of oxygen gas as a sustainable and cheap oxidant under efficient flow conditions with decatungstate anions as a selective photocatalyst.

The last example in this section is about the cerium-based photocatalyzed functionalization of low molecular weight alkanes.[43] Zuo et al. use hydrocarbons of C$_1$ to C$_4$ structure for alkylation and arylation reactions as well as for amination with di-*tert*-butyl azodicarboxylate (**37**). The principle behind this approach is the formation of cerium(IV)-alkoxides with, for example, Cl$_3$CCH$_2$OH, which are activated by visible light resulting in Ce^{III} species and alkoxy radicals. This highly electrophilic intermediate abstracts a hydrogen atom from, for example, ethane, which is subsequently converted with the nucleophilic azo compound **37** to the product **38** under recovery of the Ce^{IV} salt (Figure 10).

In the case of batch tests, good conversions of 63 to 76% could be achieved for all C$_1$ to C$_4$ hydrocarbons within 2 to 9 h reaction time. The transfer to flow mode was done with ten glass microreactors in series, each with an internal volume of 450 μL. Air-cooled LED arrays were used with an emission wavelength of 400 nm. With this setup, the reaction time could be decreased considerably to 6 min for ethane, propane, and butane, and 15 min for methane. In the latter case, pressure restrictions of the glass microreactors did not allow a higher yield than 15% in 15 min residence time. Engineering efforts are necessary here to optimize the reactor equipment for higher pressure stability, and hence better conversion. In the case of the higher alkanes, the amination of ethane (**36**) reaches the highest yield of 90% in 6 min residence time. With these results, Zuo et al. could show that the functionalization of natural gas feedstock compounds is possible with abundant Ce salts as photocatalysts. By the application of flow photoreactors, a significant reduction in reaction time could be achieved by improved gas–liquid mixing.

Chemistry–A European Journal

Review
doi.org/10.1002/chem.202000381

Chemistry Europe
European Chemical
Societies Publishing

Figure 10. Cerium-based photocatalysis with visible light enables alkane functionalization. For the batch synthesis of **39**, perdeuterated MeCN was used. For the batch synthesis of **38**, **40**, and **41**, $CeCl_3$ was used instead of $(nBu_4N)_2CeCl_6$.

2.4 Cyclization

Biologically active compounds are often complex, hetero-atom-rich polycycles with a high degree of substitution on the hydrocarbon scaffolds. In particular, the fusion of nitrogen-rich heterocycles to polycycles shows great potential for compounds with pharmaceutical applications and has attracted broad attention in the development of synthetic methodologies.[44] Jamison et al. developed a strategy for the mild synthesis of polycyclic quinoxaline derivatives from ortho-heterocycle-substituted arylisocyanides as the substrate. Phenyliodine(III)-dialkylcarboxylates were used as the alkyl radical source upon photocatalytic activation with fac-Ir(ppy)3 or Ir(ppy)2-(dtbbpy)PF6 (dtbbpy = 4,4′-di-tert-butyl-2,2′-bipyridyl, ppy = 2-phenylpyridine) as photocatalysts (Figure 11, last step). In the batch process, 1-(2-isocyanophenyl)-1H-pyrrole **44** was used as the model substrate and converted with phenyliodine(III)dicyclohexylcarboxylate and fac-Ir(ppy)3 in N,N-dimethylformamide (DMF) to the desired pyrrolo[1,2-a]quinoxaline **45** in 73% yield. The batch synthesis was done at 25 °C with a fluorescent bulb
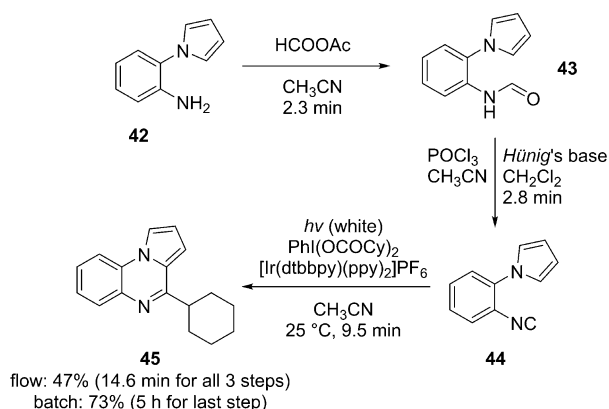
Figure 11. Three-step synthesis of a pyrrole quinoxaline derivative **45** through formamide formation, dehydration, and photochemical cyclization with carboxylated cyclohexane (dtbbpy = 4,4′-di-tert-butyl-2,2′-bipyridyl, ppy = 2-phenylpyridine).
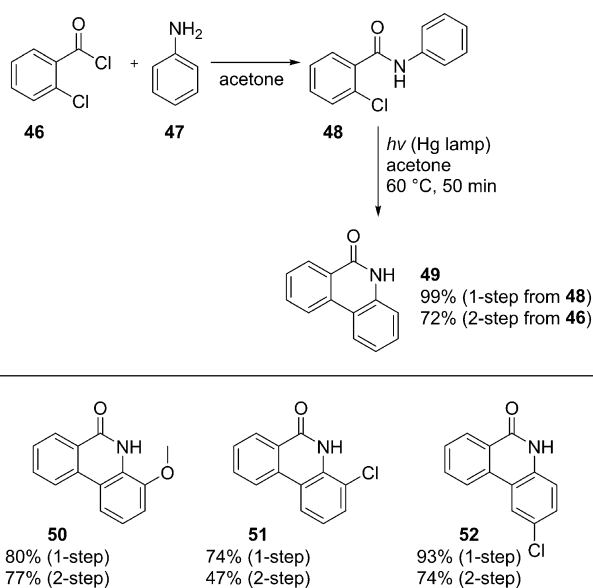
(26 W) as the light source. Based on this approach, Jamison et al. converted several pyrrole and other five-membered nitrogen-rich arylisocyanides into the respective quinoxoline derivates in moderate yields (pyrazole, 45%) to very good yields (tetrazole, 81%). The mild reaction conditions allowed the incorporation of various alkyl groups, bile acid derivatives, or amino acids.

The benefit of continuous-flow equipment was demonstrated in this work by the integration of the isocyanide formation prior to the photocatalyzed cyclization step. In the first step 2-(1H-pyrrolo)aniline **42** was converted in a capillary reactor (PFA, $\tau_{res} = 2.3$ min) with formic acetic anhydride in acetonitrile to the formamide **43**, which was subsequently dehydrated to the isocyanide **44** with $POCl_3$ and diisopropylethylamine (Hünig's base) in CH_2Cl_2 by using a second capillary reactor in line (PFA, $\tau_{res} = 2.8$ min). The crude reaction mixture containing the isocyanide, any byproducts and residual reagents was finally mixed with phenyliodine(III)dicyclohexylcarboxylate and [Ir(dtbbpy)(ppy)2]PF6 in MeCN and irradiated in a third capillary reactor (PFA, $\tau_{res} = 9.5$ min) at 25 °C. Although the desired product was obtained over all steps only in a moderate yield of 47%, the flow synthesis showed several advantages. Besides the minimized contamination of the experimenter with foul-smelling isocyanides, clever solvent and catalyst selection avoids unnecessary work-up procedures or solvent changes between each step of the continuous-flow synthesis protocol. In particular, for the photochemical step, the efficient irradiation leads to a strong reduction in reaction time from 5 or 24 h to 9.5 min.

In a second example, Tranmer et al. demonstrated the flow synthesis of 6(5H)-phenanthridinone derivatives, which have been developed for reliable access to potential poly(ADP-ribose) polymerase inhibitors.[45] The authors could show that their photochemical cyclization route is superior to the known methodologies based on the Schmidt reaction, which uses explosive HN_3, or the Ullmann and Suzuki coupling reactions, with rather moderate yields. Tranmer et al. used 2-chlorobenzamides (e.g., **48**, synthesized from benzoyl chlorides and aniline derivatives) to investigate the impact of the solvent, substrate concentration, flow rate, and type of UV light filter equipment. Optimized conditions were found with acetone as the solvent, 5 mM substrate concentration, a flow rate of $f_l = 0.2$ mL min^{-1} (FEP, 10 mL, $\tau_{res} = 50$ min), and a simple quartz glass filter with a medium-pressure Hg lamp as the light source. Under these process conditions, a broad substrate screening at 60 °C reactor temperature (Figure 12, second step) was performed. A high yield of 99% was obtained for fully unsubstituted 2-chlorobenzamide **48**. Varying the substitution pattern of the aryl groups with electron-donating methoxy groups (**50**) or electron-withdrawing chlorine atoms (**51**, **52**) gave moderate (67%) to very good yields (93%). These results are far better than any other yields reported in the literature so far.

Tranmer et al. then combined the precursory amidation reaction between 2-chlorobenzoyl chloride **46** with aniline **47** with the photocyclization reaction. The starting materials, dissolved in acetone, were pumped via a mixing T-piece into a simple

Chemistry–A European Journal

Review
doi.org/10.1002/chem.202000381

Chemistry Europe
European Chemical
Societies Publishing

Figure 12. Top: Continuous-flow synthesis of 2-chloroamide building block **48** with subsequent photocyclization to 6(5H)-phenanthridinones **49**. Bottom: Substitution patterns of the starting material determine the effective yield of the two-step synthesis. "1-step" = starting material is aryl amide, "2-step" = starting material is aryl acid chloride.

coil reactor (10 mL, $\tau_{res} = 50$ min) at 60 °C. Interestingly, no additional base like NEt$_3$ was necessary to quench the hydrogen chloride emerging from the amidation in the first step. The raw amide product solution was then directly transferred into the capillary photoreactor and converted into the desired phenanthridinones, for example, with a slightly lower yield of 77% for the methoxy derivative **50** (80%) or with an apparently lower yield of 72% for the unsubstituted phenanthridinone **49** (99%). It is worth pointing out that a lower yielding, but fast and safe multi-step flow synthesis is an important tool for a rapid drug discovery process under more sustainable conditions, as no purification of intermediates is necessary.
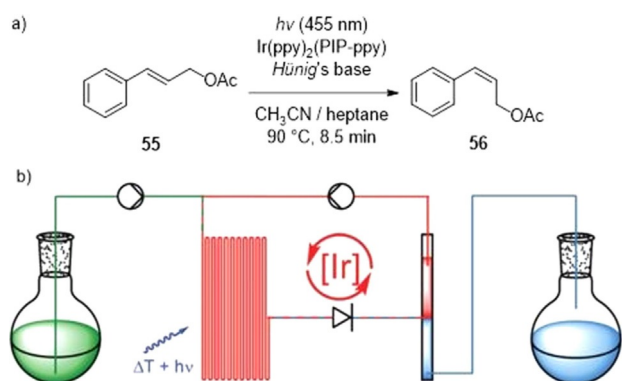
2.5 *E/Z* Isomerization

The isomerization of double bonds finds various applications in materials and biomedical science. Stilbene derivatives are known as molecular switches in polymers[46] or as anticancer drugs with only one active isomer.[47] Usually, UV light is necessary to initiate the isomerization from *E* to *Z*. To avoid numerous side reactions occurring with UV light, Rueping et al. proposed the use of an iridium complex for visible light *E*-to-*Z* isomerization of stilbene derivatives through energy transfer from the triplet state of the sensitizer to the stilbene.[48] For economic and ecological reasons, the authors used at first a two-phase batch system with ionic liquid [bmim][BF$_4$] (bmim = 1-butyl-3-methylimidazolium) as the catalyst phase for Ir(ppy)$_2$(bpy)PF$_6$ (bpy = 2,2′-bipyridine) and toluene as the substrate phase for *E*-stilbene **53**. In this combination, the expensive Ir catalyst was recycled up to eight times with a mean yield for the *Z* isomer **54** of 94% upon irradiation with a standard fluorescence lamp (11 W). For the transfer from batch to flow mode, a more effi-

cient phase separation between ionic liquid and substrate phase was necessary and was achieved by replacing toluene with *n*-pentane. *E*-Stilbene **53** (0.1 M in *n*-pentane) and Ir(ppy)$_2$-(bpy)PF$_6$ (3 mol% in [bmim][BF$_4$]) were pumped via a T-piece for premixing into a microplate glass reactor with separate mixing elements (1.1 mL, $\tau_{res} = 6.5$ min) and irradiated by a stripe of high-power LEDs at 470 nm emission wavelength (Figure 13). As desired, the phases separated immediately after leaving the glass microreactor. With this approach it was possible to directly recycle the catalyst-containing ionic liquid phase back into the process. The *Z* isomer **54** was obtained in quantitative yield, most likely owing to the excellent mixing and the strongly improved irradiation of the reaction solution inside the microstructured channel of the flow reactor.

Reiser et al. used a similar approach for the *E*-to-*Z* isomerization of cinnamyl acetate **55** with visible light.[49] The authors synthesized a polymer-bound sensitizer system based on *fac*-Ir(ppy)$_3$ with one ligand attached to a short polyisobutylene polymer chain (Glissopal 1000, n = 17). The sensitizer is soluble in apolar heptane whereas the substrate is dissolved in polar acetonitrile. Both solvents combined result in a thermomorphic solvent system, which homogenizes to a single phase at elevated temperatures greater than 85 °C. The immiscible solvent phases were mixed with a T-piece in slug flow ($f_1 = 100$ μL min^{-1} each) and transferred into a glass microreactor (1.7 mL, $\tau_{res} = 8.5$ min), which was heated to 90 °C in parallel to irradiation with blue light at 455 nm (Figure 14). A backpressure valve was set to approximately 4 bar to prevent any boiling of the solvents inside the reactor. Under these conditions,
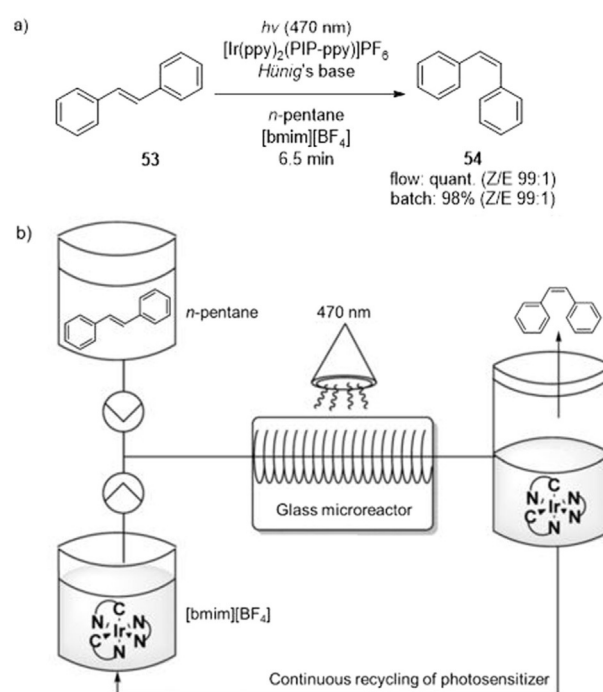

Figure 13. (a) *E/Z* isomerization of stilbene with visible light in a two-phase flow system. (b) Schematic representation of the continuous catalyst phase recycling. Reproduced with permission from ref. [48], copyright 2015 Wiley-VCH.

Chemistry–A European Journal

Review
doi.org/10.1002/chem.202000381

Chemistry
Europe
European Chemical
Societies Publishing

Figure 14. (a) *E/Z* isomerization of cinnamyl acetate **49** in continuous flow. (b) Schematic representation of temperature-controlled phase separation and catalyst recycling (ppy = 2-phenylpyridine, PIP = polyisobutylene polymer). Reproduced with permission from ref. [49], copyright 2016 Royal Society of Chemistry.

Figure 15. Continuous-flow synthesis of *E*-cyclooctenes in a microfluidic reactor setup with integrated product extraction. Reproduced with permission from ref. [51], copyright 2017 Royal Society of Chemistry.

efficient contacting between sensitizer and substrate was possible, yielding an *E*-to-*Z* isomer ratio of 18:82. After cooling down and phase separation, the apolar catalyst was cycled back into the reactor via the T-piece. The whole process performed stably for more than 25 h with constant *E/Z* ratio. Here, catalyst leaching of 2.6% took place, especially in the first two hours of this cycling process. The loss of the Ir catalyst can be attributed to the undesired solvent phase transfer of the sensitizer, bound to shorter, hence more polar polymer chains, from apolar heptane to polar MeCN. Within a further 8 h, the mean loss in Ir dropped to a low value of 0.1% and stayed constant for the residual 15 h of the process time. Reiser et al. demonstrated with this more complex approach that polymer-bound sensitizers can be constantly recycled in continuous flow and separated efficiently from a single solvent reaction phase by wise solvent selection and process parameter control. This approach is explicitly important and interesting for the recycling of expensive and rare metal catalysts like Ir.

The next example presents the reverse isomerization from *Z* to *E* for the photochemical preparation of *E*-cyclooctene derivatives. These building blocks are essentially useful for inverse electron demand Diels–Alder reactions with 1,2,4,5-tetrazines. Bormans et al. optimized a literature known methodology[50] for the light-induced *Z*-to-*E* isomerization of cyclooctenes by applying a capillary photoreactor instead of a standard batch reactor.[51] Two capillaries (FEP, each 4.1 mL) were used in parallel and wrapped around a single UV lamp (21–25 µW cm^{-2}). The reaction solution consisting of *Z*-cyclooctenol **57** as substrate (21 mM), methyl benzoate as singlet sensitizer (47 mM), and diethylether/hexane as solvent mixture (1:4) was pumped through the microcapillaries (each 5 m) and irradiated with UV light at 254 nm (Figure 15). The resulting *E/Z* mixture was then transferred to a packed bed column filled with AgNO$_3$ on SiO$_2$. The desired *E*-cyclooctenol **58** selectively binds to Ag$^+$ in the packed bed and is extracted from the reaction solution. Residual *Z*-cyclooctenol **57** is recycled back to the reservoir for further irradiation in the flow photoreactor. This approach allowed a decrease in reaction time (70%, 3.4 h) compared with
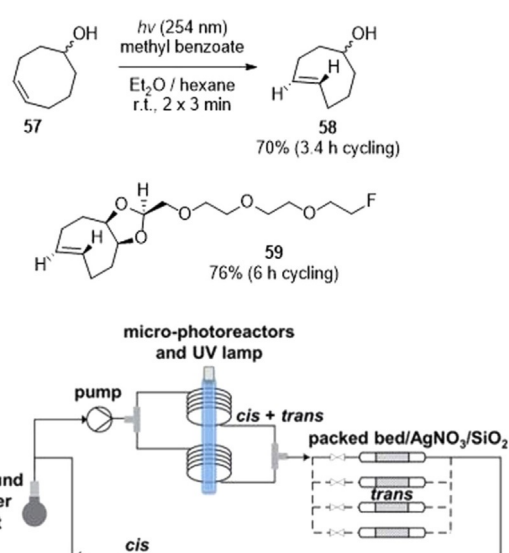
the literature procedure without irradiation in a microfluidic environment (73%, 8 h). The more complex and fluorine-containing cyclooctene derivative **59** could be obtained in 76% within 6 h of cycling.
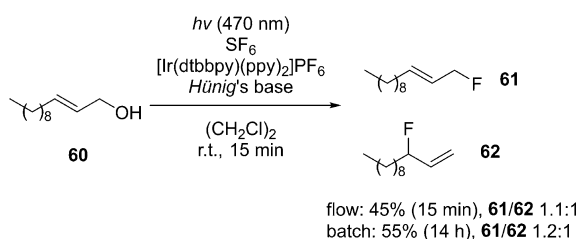
Just recently, Rutjes et al. introduced an advanced process for the *Z*-to-*E* isomerization of cyclooctenes.[52] The authors applied a slightly larger FEP capillary photoreactor with a total volume of 10.7 mL available for irradiation. Contrary to the packed bed trap containing Ag$^+$ ions, Rutjes et al. used a liquid–liquid extraction system with an aqueous silver nitrite solution against the organic heptane phase, which contains the *E* isomer enriched cyclooctene mixture. With this approach, the authors were able to provide a larger scale production of up to 2.2 g h^{-1} of *E*-cyclooctenes.

2.6 Fluorination and trifluoromethylation

Fluorinated compounds are exceptionally important for pharmaceutical and agrochemical applications. A single fluorine atom substituent or a CF$_3$ group has a strong impact on the electronic properties of a molecule and can change its lipophilicity or Brønsted acid and base characteristics, two important pharmaceutical parameters for, for example, oral bioavailability of a drug.[53] Common fluorine sources such as (diethylamino)-sulfur trifluoride (DAST) or trifluoromethyl sources like Umemoto's reagent need either cautious handling owing to its explosive character or are less used owing to their high prices.[54] Nevertheless, several methods have been developed for batch and continuous-flow monofluorinations of fine chemical building blocks. Selectfluor, a DABCO (1,4-diazabicyclo[2.2.2]octane)-based fluorination source, was used by Paquin et al. for the first photochemically catalyzed monofluorination subsequent to a decarboxylation.[55] The same reagent was used by Kappe et al. for the monofluorination of ethylbenzene as a model

Chemistry–A European Journal

Review
doi.org/10.1002/chem.202000381

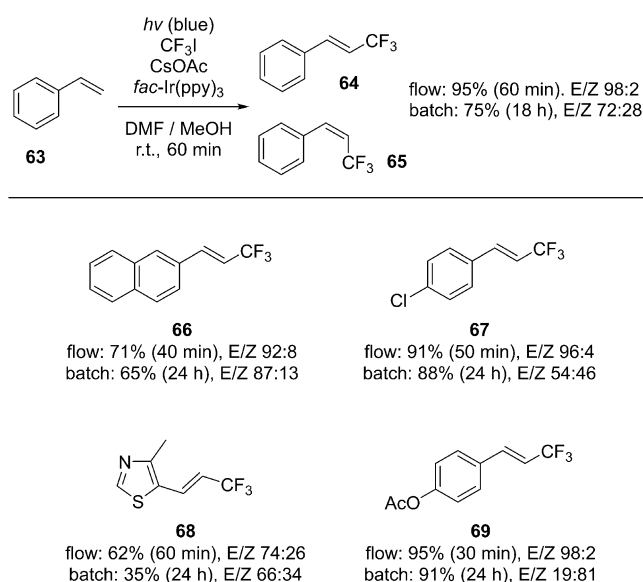**Chemistry
Europe**
European Chemical
Societies Publishing

substrate and Colestidol as industrially relevant building block for fragrance compositions.[56] A comprehensive overview on monofluorination reactions of organic compounds has been summarized by Paquin et al. in 2015.[57] In the case of single fluorination of allylic alcohols, Jamison et al. broke new ground by applying SF6, a nontoxic and inexpensive insulator gas, as the fluorinating reagent in visible light photocatalysis.[58] For the development of the desired deoxyfluorination methodology, 5-phenyl-2-penten-1-ol (0.1 mmol) was used as the model substrate for allylic alcohols with Ru(bpy)3PF6 as the photocatalyst (3 mol%) and diisopropylethylamine (Hünig's base) as a hyperstoichiometric reductant at room temperature and pressure. Several solvents were tested under these conditions with 1,2-dichloroethane, which was a superior solvent than DMSO, MeCN, or *tert*-amylalcohol. Its less polar character allows a better solubility of SF6 and most likely a better stabilization of the reactive fluorinating reagent stemming from the photoactivated SF6 radical anion. Owing to its better solubility in 1,2-dichloroethane (DCE), Ir(ppy)2(bpy)PF6 (5 mol%) was finally used as the photocatalyst with only 3 equivalents of Hünig's base as the reductant. A conversion of 96% was achieved with 55% yield and a ratio of 1.2:1 for the linear and branched isomers, respectively. The authors transferred the successful batch synthesis into flow mode by using a simple gas–liquid contacting setup consisting of a Y-mixer with a saturation loop (0.18 mL, $\tau_{res} = 1$ min) for intensifying the SF6 gas transfer into the DCE solution at approximately 6.9 bar, which was maintained with a backpressure regulator. The slug flow was then conveyed into a second capillary (2.7 mL, $\tau_{res} = 15$ min), which was irradiated with blue light at 470 nm (Figure 16). Under these conditions, 2-dodecen-1-ol **60** was converted to the desired monofluorinated compounds **61** and **62** in 45% yield (ratio linear/branched 1.1:1) compared with 55% in batch mode (ratio linear/branched 1.2:1). Although achieving a lower yield, the flow synthesis was superior in reaction time with 16 min versus 14 h in batch mode, corresponding to productivities of 0.19 mmol h^{-1} versus 0.04 mmol h^{-1}. Besides the improved productivity, the new deoxyfluorination method by Jamison et al. applies SF6 as a very safe fluorinating reagent with a nearly unbeatable price. But one should also keep in mind that SF6 is one of the most potent greenhouse gases with a global warming potential of 23900 times of CO2.[59]

The Noël group has developed a broad range of continuous-flow methodologies for the incorporation of fluorine-based functional groups as important structural motifs in mo-

lecular building blocks. Besides the perfluoroalkylation of heteroaryls[60] and trifluoromethylation of aromatic thiols,[61] a two-step flow synthesis of allylic alcohols from Grignard reagents with subsequent difluoroalkylation of the vinyl double bond was presented as well in the last years.[62] Furthermore, Noël et al. also used their expertise in the photocatalyzed activation of CF3I as an inexpensive, gaseous reagent for the trifluoromethylation or hydrotrifluoromethylation of styrene derivatives.[63] Solvent, catalyst, and base screening was done in batch mode with styrene **63** as the most simple substrate (0.5 mmol). Optimal conditions were found with DMF as solvent (0.1 mol L^{-1}), *fac*-Ir(ppy)3 as the photocatalyst (1 mol%), and cesium acetate as a mild base (2 equiv). At room temperature and pressure, **63** was converted within 18 h to the desired trifluoromethylated compounds **64** and **65** in 75% isolated yield with an *E/Z* ratio of 72:28. Furthermore, the transfer from batch to flow mode had a strong impact on both yield and reaction time. The capillary photoreactor applied was based on a standard PFA tubing (1.25 mL) and blue LEDs with an overall electrical power of 6.24 W (Figure 17). Gas–liquid contacting was done with a T-piece as a static mixing element ($f_l = 1.25$ mL min^{-1}, $f_g = 1.20$ mL min^{-1}). In the case of **63**, the yield could be increased to 95% within a residence time of $\tau_{res} = 60$ min. Equivalent results were achieved for more complex molecules **66–69** as well. Interestingly, the use of the flow photoreactor setup not only improves the productivity of the process, but affects the *E/Z* ratio as well, tending towards a higher amount of the *E* isomer. For styrene **63**, the *E/Z* ratio increased from 72:28 to 98:2. In the case of 4-acetoxysytrene conversion to **69**, the *E/Z* ratio changed even more drastically, from 19:81 in batch mode to 98:2 in continuous-flow mode. This remarkable raise in favor of the *E* isomer can be attributed to the shorter residence time in the flow photoreactor and in conse-

Figure 16. Continuous-flow deoxyfluorination of allylic alcohols with insulator gas SF6 as the fluorine source (dtbbpy = 4,4'-di-*tert*-butyl-2,2'-bipyridyl, ppy = 2-phenylpyridine).

Figure 17. Top: *E* isomer-selective trifluoromethylation of styrene (**63**) with CF3I under continuous-flow conditions (ppy = 2-phenylpyridine). Bottom: Examples demonstrating the broad scope of styrene derivatives for photocatalytic trifluoromethylation.

Chemistry–A European Journal

Review
doi.org/10.1002/chem.202000381

Chemistry
**Europe**
European Chemical
Societies Publishing

quence to a shortened irradiation time. Under these reaction conditions, the photocatalyzed isomerization of the *E* isomer to the *Z* isomer by energy transfer from the exited photocatalyst to the vinyl double bond is suppressed.[64]

For the selective hydrotrifluoromethylation of styrenes, Noël et al. changed the solvent from DMF to a mixture of DCE and ethanol (9:1, v/v) containing 1.2 equivalents of 4-hydroxythiophenol as a hydrogen atom donor (Figure 18). This reagent became necessary to avoid predominant formation of byproducts stemming from overoxidation and dimerization of the styrene substrates. Styrene **63** was converted to 3,3,3-trifluoropropylbenzene **70** with a yield of 77%, slightly lower than 79% in batch mode, but again with a strong decrease in reaction time from 24 h to 50 min in flow mode. Both methodologies allow the incorporation of trifluoromethyl groups into a broad variety of styrene derivatives or vinyl group containing substrates under very mild conditions.
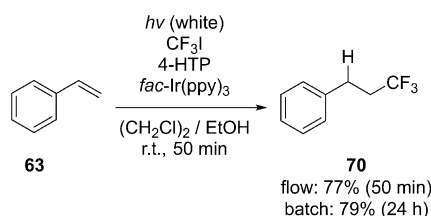
Figure 18. Hydrotrifluoromethylation of styrene derivatives with 4-hydroxythiophenol (4-HTP) as a hydrogen atom donor (ppy = 2-phenylpyridine).

In the last example, Stephenson et al. give a rare example for the development of a new synthesis process in flow, which also includes a detailed protocol for the transfer from milligram quantities to kilograms. In the first work, the authors introduced the combined use of trifluoroacetic acid anhydride (**72**) and pyridine *N*-oxide together with Ru(bpy)₃Cl₂ as photocatalyst as a broadly applicable reagent mixture for the trifluoromethylation of various arene building blocks.[65] Selective cleavage of the anhydride by pyridine *N*-oxide results in the ionic adduct formation of 1-[(trifluoroacetyl)oxy]pyridinium trifluoroacetate, which can be easily reduced by the sensitizer and converts into the desired CF₃ radical, CO₂, and pyridine. Various vinyl, aryl, and heteroaryl substrates were converted to the respective CF₃-containing compounds in low (17%) to moderate yields (74%). In the case of *N*-Boc (*tert*-butyloxycarbonyl) pyrrole **71**, scale-up attempts have been performed as well. On the lab scale, this heteroarene was converted in batch mode to the single and double trifluoromethylated product (ratio 1:1) with 74% yield. On the 5 g batch scale, only 53% yield was obtained with a single to double substitution pattern of 4:1. On the 18 g scale, the yield was comparable with 57%, whereas on the 100 g scale the yield was as low as 35% even after 62 h instead of 15 h. The transfer to flow mode resulted in a yield of 71% on the 20 g scale at a residence time of only $\tau_{res} = 10$ min. On the basis of this very positive result, Stephenson et al. employed the continuous-flow synthesis on a kilogram scale (Figure 19).[66] A common capillary photoreactor was used (PFA, 150 mL) with three underwater LED light sourc-
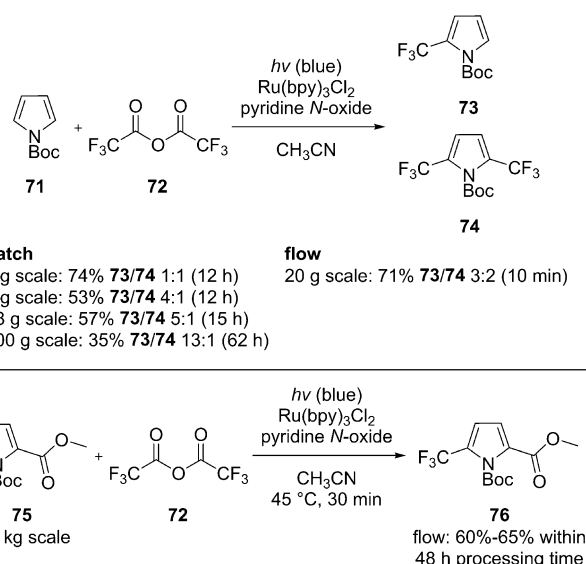
Figure 19. Top: Batch and flow evaluation for trifluoromethylation of pyrrole compound **65** with TFAA as source of trifluoromethyl radicals. Bottom: Real process scale-up for the trifluoromethylation of 1.2 kg of pyrrole derivative **75** (bpy = 2,2′-bipyridine).

es for blue light irradiation. The complete system was cooled with water to a temperature of 45 °C. With this setup, 2-methyl *N*-Boc pyrrole-2-carboxylate **75** (5.33 mol, 1.2 kg!) was converted with 0.1 mol% Ru(bpy)₃Cl₂ and 2 equivalents of the trifluoroacetic acid anhydride (TFAA)/pyridine *N*-oxide adduct to the desired trifluoromethylated pyrrole building block **76** with a yield of up to 65% during 48 h of process time, which corresponds to a substrate consumption of 25 g h⁻¹ and 111 mmol h⁻¹, respectively. After workup of the raw material, a final productivity of 87.2 mmol h⁻¹ was obtained, which outperforms the previous batch (4.2 mmol h⁻¹) and flow syntheses (14.2 mmol h⁻¹) by a factor of up to six. Surely, this work by Stephenson et al. is an outstanding example that large-scale flow photochemistry is growing out of its infancy.

2.7 Arylation via diazonium salts and diazo compounds

The conversion of amines into their corresponding diazonium salts is an attractive route for the activation of carbon atoms towards bond formation with other (hetero)atoms.[67] Besides well-known metal-catalyzed coupling reactions with diazonium salts as starting materials, light-mediated syntheses have been developed as well in recent years.[68] Just recently, Ackermann et al. published their work on arene C—H activation in flow by using a photocatalyst based on manganese as an earth-abundant metal.[69] In the case of carbon–sulfur bond formation, Noël et al. developed a mild and biocompatible, that is, metal-free arylation method for the amino acid cysteine.[70] Based on their prior investigation of the Ziegler–Stadler reaction for the photochemical synthesis of thioether derivatives,[71] Noël et al. performed batch screening reactions regarding diazonium salt formation, solvent, sensitizer, and light source. N,C-Protected cysteine **77** was arylated with 4-fluoroaniline **78** in 46% yield by using *t*BuONO and *p*-toluenesulfonic acid for in situ diazoti-

Chemistry–A European Journal

Review
doi.org/10.1002/chem.202000381

Chemistry Europe
European Chemical
Societies Publishing

zation, acetonitrile as solvent, Eosin Y as the metal-free sensitizer, and a compact fluorescent lamp as the light source. The transfer to continuous-flow mode was done by using a capillary photoreactor (PFA, 450 µL) and a white light LED array ($P_{ele} = 3.12$ W). tBuONO (0.2 M in acetonitrile) was mixed via a T-piece with an acetonitrile solution containing N-Ac-L-cysteine-OMe **77** (0.1 M), eosin Y (1 mol%), p-fluoroaniline **782** (0.13 M), and p-toluenesulfonic acid (4 mol%) before entering the irradiated capillary. Within a very short residence time of $\tau_{res} = 30$ s, the N,C-protected amino acid was converted to the desired thioether **79** in 79% yield (Figure 20). By using these optimized flow conditions, various aniline derivatives were converted in situ into diazonium salts for subsequent coupling with the thiol group of cysteine. In the case of unsubstituted aniline, the yield was increased by 22 to 72% for the flow synthesis. For 4-ethynylaniline, a prolonged residence time of $\tau_{res} = 60$ s was necessary to reach 61% yield compared with 49% yield in 2 h for the batch reaction. As a representative of dipeptides, Leu-Cys was converted with 4-trifluoromethylaniline to the corresponding thioether **82** in 86% yield (flow mode) and 61% yield (batch mode).
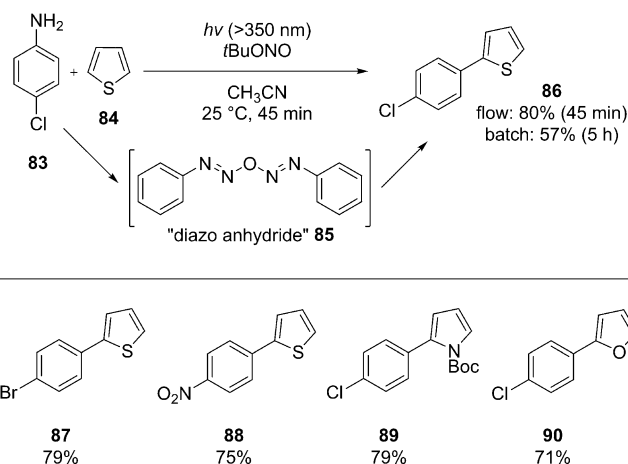
In another example, Kappe et al. did not use an in situ formed diazonium salt, but the corresponding diazo anhydride **85**, which is the self-condensation product of arylnitrosamine and arylhydroxydiazene, both intermediates occurring during diazonium salt formation.[72] These anhydrides are known to decompose into aryl radicals, which can be promoted by light with a wavelength greater than 300 nm. Kappe et al. used this concept for the intensified flow synthesis of various bi(hetero)-aryls. For example, 4-chloroaniline **86** (0.4 M) and thiophene **84** (8 equiv) were mixed with tBuONO (1.2 equiv) in a T-piece before entering the capillary photoreactor. UV light was supplied by a mercury lamp with a filter blocking wavelengths below 300 nm. Within a residence time of $\tau_{res} = 45$ min, the
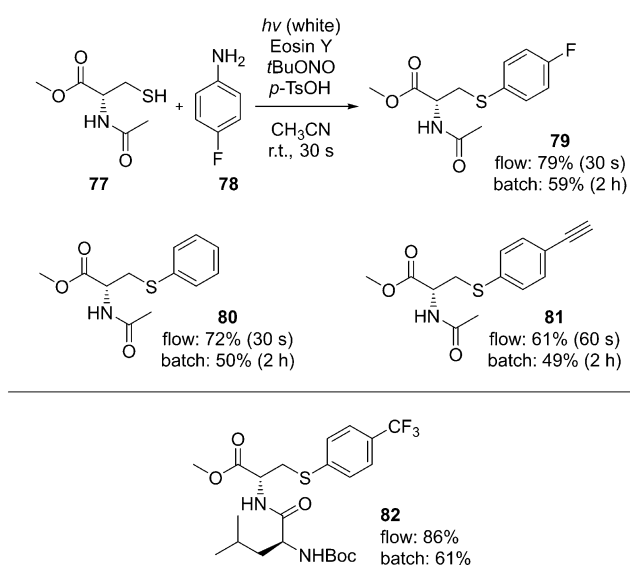
mixture was converted to 2-(4-chlorophenyl)thiophene **80** in 80% yield compared with 57% in batch mode with 5 h reaction time (Figure 21). Electron-deficient anilines were converted in good yields (**87**, **88**). Electron-rich anilines or bulky groups close to the amino function hinder the reaction most likely by the side-reaction between aryl radicals and residual aniline starting material. Other heteroarenes like N-Boc pyrrole or furan are converted as well in good yields of 79% for **89** and 71% for **90**. The synthetic method of Kappe et al. is an interesting example for a photochemical conversion of an in situ formed and labile, but photoactive species, which could be intensified under flow conditions to higher yields in shorter reaction times.

Besides charged diazonium salts, neutral diazo compounds also play a pivotal role in organic synthesis. Usually, diazoalkanes are stabilized by electron-withdrawing groups or π-systems in close proximity to the diazo group. In contrast, non-stabilized diazoalkanes, like diazomethane, must be prepared in situ for safe handling.[73] Ley et al. recently developed a method for the photochemical synthesis of diazo compounds made from oxadiazolines as safe precursors for diazoalkanes.[74] The authors applied a literature-known methodology from Warkentin et al., who describe the selective photolysis of 1,3,4-oxadiazolines (**92**) with UV light at approximately 300 nm into diazoalkanes (**93**) and alkylacetate.[75] Importantly, the synthesis of oxadiazolines is a straight-forward one-pot, two-step procedure with a broad variety of ketones available as the starting materials. Ley et al. combined these advantages for the photochemical in situ formation of various unstabilized diazoalkanes and their subsequent conversion with para-substituted arylboronic acids. For example, 4-chlorophenylboronic acid **91** (0.05 M in dichloromethane), oxadiazoline **92** (2 equiv), and diisopropylethylamine (Hünig's base, 2 equiv) were pumped as one solution into a capillary photoreactor (FEP, 10 mL, $\tau_{res} =$ 80 min), which was cooled to 10 °C and irradiated with UV light at 310 nm (9 W). Inline IR analysis was used to monitor the reaction with the C=O stretch band of methyl acetate at

Figure 20. Top: Biocompatible arylation of cysteine's thiol group in **77** via in situ formed diazonium salts with subsequent photocatalyzed activation. Bottom: N-Boc-L-Leu-L-Cys-OMe in **76** as an example of a dipeptide for selective arylation of a thiol group.

Figure 21. Top: Proposed diazo anhydride formation in the photochemical reaction pathway of light-induced C—H arylation of arenes. Bottom: Examples for arene and heteroarene substrate scope for photocatalytic C—H arylation.

Chemistry–A European Journal

Review
doi.org/10.1002/chem.202000381

Chemistry Europe
European Chemical
Societies Publishing

1746 cm^{-1} as a probe for the successful photolysis of the oxa-diazoline. The resulting product solution, containing the desired tertiary boronic acid **94**, was not isolated, but stirred either with TBAF (3 equiv) or under air atmosphere (Figure 22). In the first case, B(OH)$_2$ was substituted with a hydrogen atom in 71% overall yield for **95**, in the second case, with a hydroxy group in 76% overall yield for **96**. This mild synthesis method allows the conversion of diazoalkanes functionalized with, for example, C—C triple and double bonds (85% for **97** and 89% for **98**). Diazoalkanes based on O-, N-, or S-heterocycles and carbocycles (as 4-, 5-, and 6-membered ring systems) are converted smoothly as well (**99**, **100**). In addition, the substitution pattern of the aryl boronic acid can be varied as well with, for example, CF$_3$ (68% for **101**) or NHAc (88% for **102**) instead of a chlorine atom. Finally, the tertiary boronic acid was also trapped as a pinacol ester for further derivatization in other reactions, for example, for the construction of a quaternary carbon center in **103** through the conversion with 2-lithiofuran in 47% yield. Ley et al. have developed a mild and very powerful method for the metal-free cross-coupling of C(sp^2) and C(sp^3) centers by using the photochemical in situ formation of unstabilized diazoalkanes under safe and excellently controllable flow conditions.
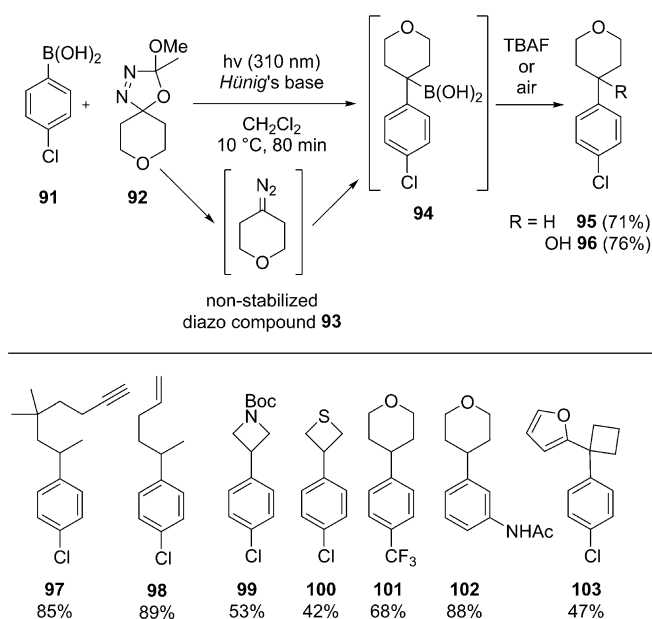
Figure 22. Top: Easy access to unstabilized diazo alkanes via flow photolysis of oxadiazolines **92** with excellent functional group tolerance (TBAF = tetra-butylammonium fluoride). Bottom: Examples for arene and heteroarene substrate scope for photocatalytic C—H arylation.
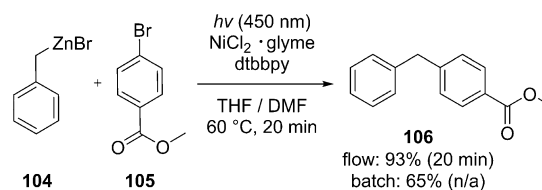
2.8 Light-induced cross-coupling reactions

In analogy to photocatalyzed arylation reactions with diazonium salts, novel variations of classical transition metal cross-coupling reactions have been developed as well. For instance, dual-catalysis approaches apply Ru or Ir complexes as photosensitizers together with another organometallic catalyst for the bond formation.[21] Unfortunately, rare earth metals make

this route less sustainable and cost-effective for process scale-up. To overcome this issue, Alcázar et al. developed a photosensitizer-free Negishi cross-coupling protocol based on earth-abundant metal complexes of Zn and Ni.[76] The authors performed first batch tests with methyl 4-bromobenzoate **105** (0.1 M) and readily available benzylzinc bromide **106** (0.2 M) with fac-Ir(ppy)$_3$ as the photosensitizer (1 mol%) and various Ni-based complexes as cross-coupling catalysts. Blue light irradiation in a commercially available 24-vial photoreactor yielded conversions between 26% (Ni(cod); cod = 1,5-cyclooctadiene) and 65% (NiCl$_2$·glyme, dtbbpy) to the desired product. Tests of the same reaction were then transferred to continuous-flow mode with a flow rate of $f_l = 250\ \mu L\,min^{-1}$ for each stream combined in a T-mixer prior to the inlet of a commercially available capillary photoreactor ($\tau_{res} = 20$ min). Roughly the same maximum conversion of 64% was obtained with Ni(dtbbpy)Cl$_2$ as the cross-coupling catalyst. Surprisingly, the omission of the Ir photosensitizer resulted in a higher conversion of 70%. Without irradiation at 450 nm, the conversion dropped to 4%. In contrast, full conversion could be achieved by combining visible light with a reaction temperature of 60 °C (Figure 23). Spectral analysis of the reaction solution and the single compounds revealed a significant absorption band in the visible region for the Ni^{2+} complex with dtbbpy and the organozinc compound in the ligand sphere. Basic mechanistic investigations point to a visible light accelerated reduction of Ni^{2+} to Ni^0 in a first step and an acceleration of the reductive elimination within the catalytic cross-coupling cycle by blue light absorption.

In addition to the continuous-flow cross-coupling reaction, the authors also used a novel continuous-flow protocol for the on-demand preparation of organozinc halides used in this work.[77] Especially in the case of 4-bromoanisole, a building block, which is usually not applied to Ni-catalyzed Negishi coupling, the fresh preparation of the organozinc halide was essential and resulted in 53% conversion to the cross-coupling product, whereas the commercially available zincate reagent did not even react. Based on the flow protocol developed by Alcázar et al., a broad range of bromo- and iodo- as well as chloroarenes were converted to bis(hetero)aryl compounds. Most of the presented examples clearly benefit from blue light irradiation resulting in an increase in conversion of up to 90%.

Alcázar et al. also published their work on the scalability of light-induced Negishi cross-coupling reactions.[78] A commercially available pilot-scale continuous-flow photoreactor was applied to the synthesis of trifluoromethoxylated phenylben-

Figure 23. Negishi cross-coupling reaction with in situ formed visible light absorbing Ni/Zn complexes for accelerated C(sp^3)—C(sp^2) bond formation (dtbbpy = 4,4'-di-tert-butyl-2,2'-bipyridyl).

Chemistry–A European Journal

Review
doi.org/10.1002/chem.202000381

Chemistry Europe
European Chemical
Societies Publishing

zoate **107** and 5-benzylpyrimidin-2-amine **108** (Figure 24). The goal of this work was to outline the possibility for the on-demand synthesis of potential APIs for preclinical medical programs with a suitable scale of several $10 \, g \, day^{-1}$. In the case of **107**, the throughput was increased by a factor of seven to $5.6 \, g \, h^{-1}$, which corresponds to a daily production of more than 130 g. In the case of **108**, a factor of 11 was achieved, yielding $3.4 \, g \, h^{-1}$ or more than $80 \, g \, day^{-1}$.

107
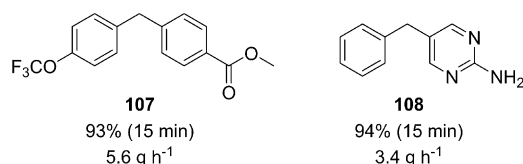93% (15 min)
5.6 g h⁻¹

108
94% (15 min)
3.4 g h⁻¹

Figure 24. Potential APIs via scaled-up light-induced Negishi cross-coupling.

Moreover, the authors also applied modern process analytical technology by the incorporation of a benchtop NMR spectrometer, which was adapted to continuous-flow mode with a simple PTFE tube as a flow cell (Lamor frequency for ^1H: 43 MHz). Inline ^1H NMR analysis was used to monitor the progress in organozinc halide formation with the benzyl CH_2 group as a probe. In summary, the work of Alcázar et al. is an impressive proof for the straight-forward combination of continuous-flow synthesis with solid materials like zinc, light-induced conversion of in situ formed metalorganic intermediates, and innovative analytical tools for process control.

In analogy to the Ni-mediated Negishi C–C coupling, Noël et al. also developed a sustainable continuous-flow method for the C–C Kumada coupling of alkyl Grignard reagents with aryl chlorides using Fe complexes, in situ built with imidazolium ligands.[79] Irradiation with blue light accelerates the C–C coupling reaction considerably as shown by the increased product formation of, for example, cyclohexylbenzene from benzene chloride (**109**) and cyclohexyl magnesium chloride (**110**, Figure 25). Within a short residence time of 5 min, the yield in-
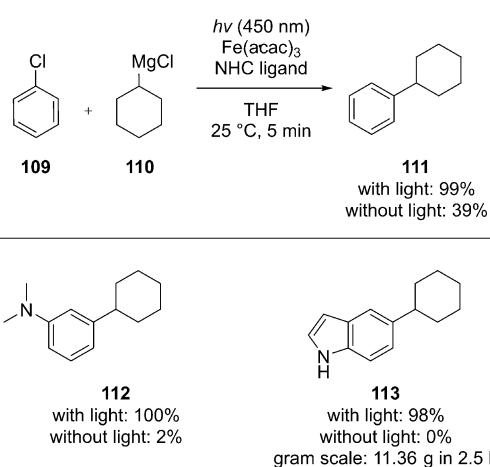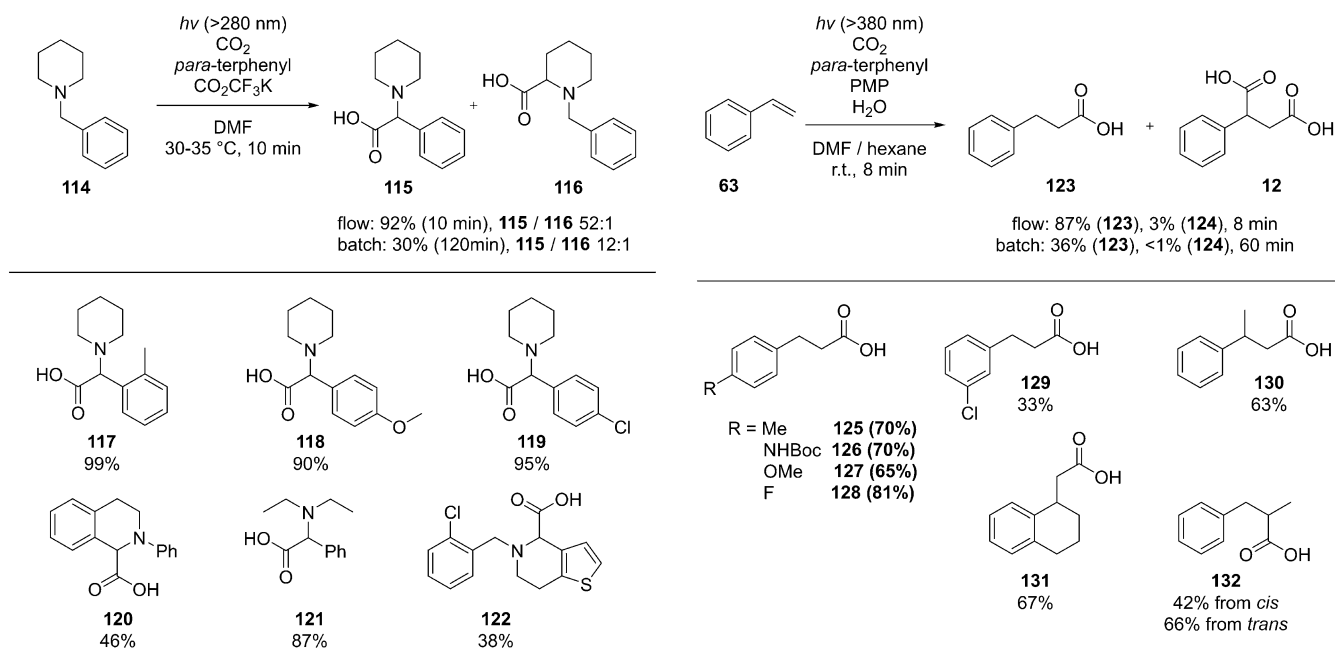
creased from 39% without light to 99% with blue light irradiation. An even stronger tendency could be shown by the use of electron-rich aryl chlorides like N-methylated anilines or indole, which previously needed high temperatures and long reactions times. N,N-Dimethylated chloroaniline could be fully converted to **112** (2% without light), 5-chloroindole yielded **113** in 98% although there was zero conversion without light. Importantly, the latter process could be easily scaled-up to the multigram scale of approximately 12 g in 2.5 h, which corresponds to a space time yield of $454 \, mg \, h^{-1} \, mL^{-1}$. These results clearly show the highly relevant expansion of the Kumada C–C coupling with light in continuous flow.

2.9 Activation of CO₂

Carbon dioxide is a highly attractive C_1 building block for chemical synthesis owing to its general availability from the natural photosynthetic cycle or by the emission from anthropogenic sources. The high stability of CO_2 is reflected in the low reactivity of this feedstock gas, which limits its application in mild synthesis methods.[80] Contrary to the usually applied two-electron chemistry, Jamison et al. combined a mild photoredox process with continuous-flow technology for the selective one-electron reduction of CO_2 in the synthesis of amino acids.[81] For CO_2 activation, a high reduction potential of $E^0 = -2.21 \, V$ in DMF (vs. saturated calomel electrode, SCE) is necessary, usually enhanced with an overpotential of 0.1–0.6 V. This challenging reaction condition rules out the standard photoredox catalysts containing Ru or Ir as ligand centers. Based on the prior work by Yanagida et al.,[82] the authors decided to use *para*-terphenyl as a sensitizer (20 mol%) with a reduction potential of $E^0 = -2.63 \, V$ in DMF (vs. SCE) and a maximum absorption band at $\lambda_{max} = 283 \, nm$. For process development, N-benzyl piperidine **114** was used as the substrate, potassium trifluoroacetate (3 equiv) as a base, and DMF as the solvent (Figure 26). Efficient gas–liquid contacting was achieved in slug flow with a T-piece mixer prior to the inlet of the capillary photoreactor. A UV light source was integrated in the reactor with a cut-on filter for irradiating the reaction solution with light of wavelengths greater than 280 nm. At a system pressure of 3.4 bar and a residence time of $\tau_{res} = 10 \, min$, **114** was converted to the carboxylic acids **115** and **116** in 92% yield with a regioselectivity of 52:1 in favor of **115** with the carboxylic acid in the benzylic position. Comparative batch experiments with CO_2 bubbled through the solution resulted in a yield as low as 30%. With these conditions in hand, Jamison et al. used the continuous-flow setup to convert N-benzyl piperidine derivatives with various substitution patterns at the aryl core into the desired amino acids. Methyl substitution in the *ortho*-position results in an excellent yield of 99% for **117**, methoxy substitution still gives 90% yield for **118**. The yields for chloro-substituted benzylamines is highly dependent on the position of the chlorine atom: 58% for *ortho*-, 85% for *meta*-, and 95% yield for *para*-substitution in **119**. Carboxylated isoquinoline **120** was obtained in 46% yield. Acyclic benzylamines like N,N-diethylbenzylamine can be converted as well in a good yield of 87% for **121**. A more complex molecule like ticlopidine, an

hv (450 nm)
Fe(acac)₃
NHC ligand

THF
25 °C, 5 min

109   **110**

111
with light: 99%
without light: 39%

112
with light: 100%
without light: 2%

113
with light: 98%
without light: 0%
gram scale: 11.36 g in 2.5 h

Figure 25. Blue light accelerated Kumada coupling with enhanced substrate scope in electron-rich aryl chlorides.

Chemistry–A European Journal

Review
doi.org/10.1002/chem.202000381

Chemistry Europe
European Chemical
Societies Publishing

Figure 26. Top: α-Carboxylation of amines with photoredox-activated CO_2 performed in a continuous-flow photoreactor. Bottom: Examples of the amine substrate scope for photocatalytic amino acid synthesis with CO_2.
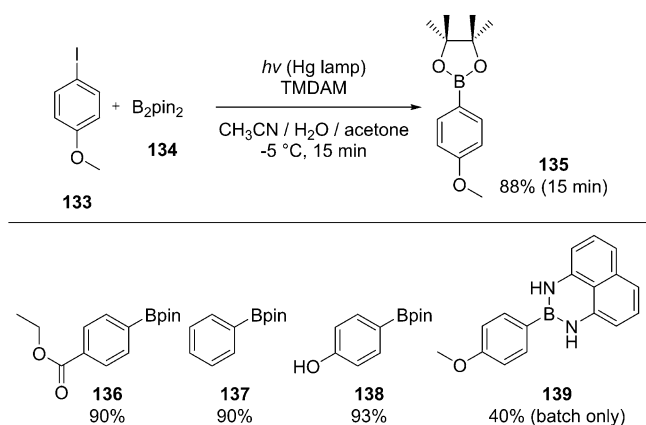
Figure 27. Top: Highly β-selective hydrocarboxylation of styrenes by *p*-terphenyl photocatalyzed CO_2 activation in continuous flow (PMP = 1,2,2,6,6-pentamethylpyridine). Bottom: Examples of styrene substrate scope for photocatalytic carboxylic acid synthesis with CO_2.

anti-platelet agent, was converted to **122** with a yield of 38% as a single regioisomer. In particular, this last example shows the potential of the mild photoredox activation of CO_2 for late-stage functionalization approaches.

In another example, Jamison et al. used photoredox CO_2 activation for the hydrocarboxylation of styrene derivatives.[83] Importantly, the reactive CO_2 radical anion from the photoredox cycle leads to the formation of the anti-Markovnikov product. This selectivity stems from the addition of the $CO_2^{\cdot-}$ to the β-position of the vinyl group, which generates in consequence a stable benzylic radical. This pronounced β-selectivity is in clear contrast to noble metal catalyzed hydrocarboxylation reactions, which yield the Markovnikov product (α-selectivity). Process development resulted in optimized reaction conditions for the *p*-terphenyl photocatalyzed (20 mol%) hydrocarboxylation with 1,2,2,6,6-pentamethylpiperidine (PMP, 2 equiv) as the reductant and 19 equivalents of water as the proton source in a DMF/hexane solvent mixture (3:1). This additive/solvent combination became necessary to prevent any clogging of the capillary reactor owing to byproduct precipitation. With these conditions, styrene **63** (0.142 M) was converted within a residence time of $\tau_{res} = 8$ min to 3-phenylpropanoic acid **123** in 87% yield at atmospheric CO_2 pressure in the flow system (Figure 27). The diacid byproduct **124** was obtained in 3% yield. The batch-mode synthesis yielded only 36% of the desired product with a very small amount of diacid byproduct (below 1%).

Jamison et al. then investigated a broad range of core-substituted styrene derivatives. Moderate to good yields were obtained for electron-rich to electron-neutral substituents at the styrene core (**125–129**). In the case of α-substituted styrenes, only monocarboxylated products were obtained, for example,

3-phenylbutanoic acid **130** (63%) or 1,2,3,4-tetrahydro-naphthalen-1-ylacetic acid **131** (67%). Styrenes with β-substitution such as *cis*- or *trans*-1-phenylpropene were converted to the corresponding monoacid **132** in 42% and 66% yield, respectively, with very low diacid byproduct formation. The work of Jamison et al. highlights the possibilities of photochemistry as an orthogonal synthesis route to metal-catalyzed reaction pathways with opposite product selectivity. Furthermore, flow technology demonstrates an advanced synthesis process with strongly increased conversion for the β-selective hydrocarboxylation of a broad range of styrene derivatives.

2.10 Borylation

Arylboronic acids are commonly used building blocks in synthetic organic chemistry with special focus on carbon–carbon and carbon–heteroatom bond formation.[84] In addition to usually applied synthesis routes via Grignard or Li reagents, metal catalysis, or noble metal-free catalysis, Li et al. developed an efficient photochemical route for the borylation of aryl halides.[85] For the reaction optimization in batch mode, *p*-iodoanisole **133** (0.1 M) was used as the model substrate with bis(pinacolato)diboron **134** as the borylation reagent (2 equiv). Bis(dimethylamino)methane (TMDAM) was used as an additive (50 mol%) and 0.9 M acetone in acetonitrile/water (4:1) as a complex solvent system (Figure 28). The reaction mixture was placed in a quartz test tube and irradiated for 4 h at room temperature with a high-pressure Hg lamp (300 W) at a maximum emission of 365 nm. Strong UV irradiation results in the formation of an aryl radical. Homolytic cleavage of the carbon–iodide bond in the excited aryl iodide is proposed by the authors as well as the decomposition of an aryl iodide radical

Chemistry–A European Journal

Review
doi.org/10.1002/chem.202000381

Chemistry Europe
European Chemical
Societies Publishing

Figure 28. Top: Efficient borylation by photolysis of aryl halides as the activation step (pin = pinacol, TMDAM = N,N,N′,N′-tetramethyldiaminomethane). Bottom: Examples of the arene scope for the photolytic borylation with different borylation reagents.

anion, which stems from a single electron transfer from the amine additive. Radical cleavage of the protonated borylation reagent by the aryl radical then leads to the desired product **135** in 81% yield at 94% conversion. Here, anisole is the major byproduct through deiodination in 10% yield. These excellent results were even outperformed by the transfer of the developed synthesis route to continuous-flow mode. Li et al. used a standard FEP capillary (780 μL) wrapped around an immersion well, which was equipped with the Hg lamp already used. This setup allowed full conversion after a short residence time of $\tau_{res} = 15$ min at $-5\,°C$ with 88% yield for the pinacol-protected boronic acid **135** and 4% yield for anisole as the byproduct from dehalogenation. These final flow conditions also allowed a reduction of the borylation reagent to 1.5 equivalents as it was rapidly consumed in the flow reactor and did not decompose as it was the case under batch conditions with a prolonged irradiation time.

Li et al. screened a broad variation of aryl iodides and bromides by applying their novel borylation route. As a representative example for aryl iodides, ethyl 4-iodobenzoate was converted to **136** in 90% yield under flow conditions whereas only 81% yield was possible in batch mode. The less reactive ethyl 4-bromobenzoate yielded 78% product in flow mode. Gram-scale borylation was performed with iodobenzene and p-iodophenol in a commercially available reactor system with 7.8 mL capillary volume. The desired arylboronate products were obtained with excellent yields of 90% for **137** and 93% for **138**. Li et al. broadened their photochemical borylation method also to other borylation reagents like bis-boronic acid, bis(neopentanediolato)diboron or even unsymmetrical (pinacolate)-(diaminonaphthalene)diboron. In the latter case, the diaminonaphthalene boronate substituent was introduced selectively (**139**). It should be noted that in a later work the authors presented their results on the continuous-flow photolysis of electron-rich arylchlorides and fluorides as well as various aryls with mesylate, triflate, and diethyl phosphate groups used as pseudo halides for radical cleavage.[86]

The incorporation of more than one boronate group into an aromatic system leads to highly interesting aryl buildings blocks with multiple sites for coordination[87] or further synthetic manipulation.[88] A novel methodology for a regioselective C–H/C–X diborylation of iodo-, bromo-, and chloroaryls with B₂pin₂ (pin = pinacolato) was developed by Larionov et al.[89] The additive- and metal-free photoinduced process allows the straightforward synthesis of 1,2- or 1,3-diborylated aryls depending on the choice of the solvent and the position and electronic properties of other substituents in the aryl halogen substrate (Figure 29). In the case of a medium polar solvent like 2-propanol, the 1,2-regioisomer is favored, whereas highly polar hexafluoro-2-propanol directs the reaction pathway towards the 1,3-isomer. Furthermore, the authors point out that, if a strong electron-withdrawing substituent is present in the para-position or a strong electron-donating substituent is present in the meta-position, 1,2-diborylation also becomes dominant in hexafluoro-2-propanol.

A broad substrate scope was investigated in both batch (quartz glass tube, 15 °C) and continuous flow (FEP capillary reactor, 111 mL, $f_l = 0.5$ mL min⁻¹, $\tau_{res} = 222$ min, 25 °C) according to this novel photolysis protocol using light sources with a predominant UV emission wavelength of $\lambda_{max} = 254$ nm. In general, 1,3-diborylations gave slightly better yields on a small scale, whereas the flow synthesis offered a strongly reduced reaction time. 2-iodotoluene **140** was converted to the desired diborylated aryl **141** with a yield of 78% in batch mode (0.6 mmol, 14 h) and 74% in flow mode (11.5 mmol, 3.7 h). The same ratio has been found for **142** and **143**. The influence of the substitution pattern, for example, switching from meta-substituents to para-substituents, resulted in a more efficient 1,2-diborylation in flow than in batch mode for the latter two cases. Hence, the
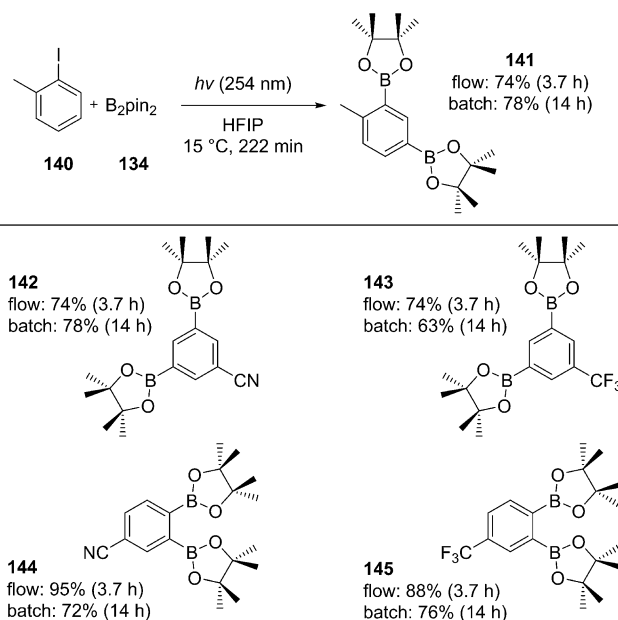

Figure 29. Top: Selective dual C–H/C–X borylation of aryl halogens by photolysis with UVC radiation in batch and flow mode (pin = pinacol, HFIP = 1,1,1,3,3,3-hexafluoro-2-propanol). Bottom: Examples of CF₃- and CN-substituted arenes with two borylate groups in the 1,2- and 1,3-positions.

conversion of 4-iodobenzonitrile to **144** gave a yield of 72% (0.6 mmol, 14 h) in batch and 95% (10.9 mmol, 3.7 h) in flow. With 1-iodo-4-(trifluoromethyl)benzene, the batch synthesis yielded 76% (0.6 mmol, 14 h) whereas the flow synthesis gave 88% of the desired diborylated aryl compound **145** (7.4 mmol, 3.7 h). Both products were obtained as single isomers without contamination from other isomers. These results confirm that the development by Larionov et al. offers a very interesting synthesis platform for the dual borylation of multiple substituted aryls. Furthermore, flow chemistry allows higher yields only in part, but a more productive synthesis process in general.

2.11 Rearrangements

The reaction class of rearrangements is often part of complex synthesis routes for natural products.[90] As an interesting variant to the well-known Beckmann rearrangement, Lattes and Aubé introduced and studied a two-step synthesis route starting from a ketone, which is converted into an oxazaridine with subsequent photolytic rearrangement into the desired lactam.[91] Based on this work and their knowledge about the benefit of continuous-flow technology on photochemical synthesis, Cochran et al. investigated and optimized the photolytic rearrangement of chiral oxaziridines in a capillary photoreactor for scale-up.[92] For process development and optimization, prochiral 4-tBu-cyclohexanone was transformed in batch mode to the corresponding imine with S-α-methyl-benzylamine heated in toluene. The diastereomeric product was then oxidized with m-chloroperbenzoic acid (m-CPBA) to the desired oxazaridine **146**. The photochemical rearrangement was finally done in a three-layer capillary photoreactor (FEP, 130 mL) with a medium-pressure Hg lamp as a light source without filter equipment (450 W). The temperature was maintained at room temperature with a cold stream of nitrogen gas around the capillary reactor placed inside a Dewar flask. The reaction solution (0.1 M in acetonitrile) was pumped through the capillary with a flow rate of $f_l = 5$ mL min^{-1} ($\tau_{res} = 26$ min). On the 1 g scale, the process yielded 82% isolated S isomer **147** whereas only 70% yield was possible in a 6 h batch reaction (Figure 30).
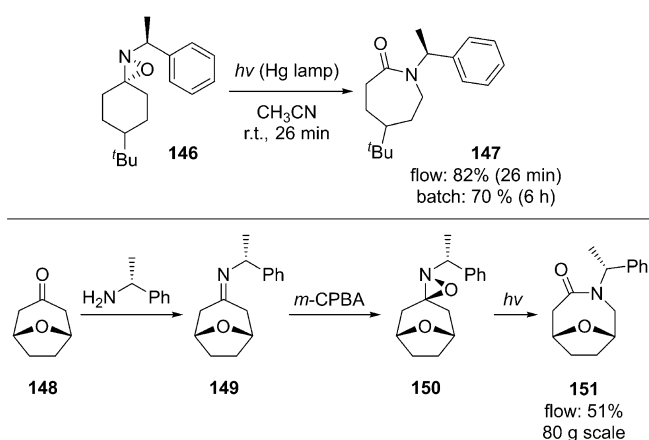
With the optimized reaction conditions at hand, Cochran et al. also performed a scale-up of the same synthesis, obtaining 20 g of the desired lactam with a yield >80%.

Finally, the authors also investigated the rarely known conversion of bicyclic ketones to the corresponding lactam. Oxabicyclooctanone **148** was converted with R-α-methyl-benzylamine to the imine **149**, which was subsequently oxidized with m-CPBA to the oxaziridine **150** as a single diastereomer in 51% yield. Photolytic treatment was done on 80 g scale. Unfortunately, the conversion of the bicyclic oxaziridine proceeded significantly slower, resulting in only 51% yield for **151** (approx. 40 g of product). However, the residual starting material could be recovered by chromatographic separation yielding effectively 99% of the chiral lactam in the end.

In analogy to the formation of lactams, also non-cyclic amide groups can be obtained by the photolytic rearrangement of oxaziridines. Jamison et al. developed a synthetic methodology based on the formation of nitrones from amino acid-based hydroxyl amines and aldehydes. Nitrone **152** is photochemically converted to oxaziridine **153**, which subsequently rearranged to the amide group in **154** after homolytic photolysis of the nitrogen–oxygen bond and subsequent hydrogen atom migration (Figure 31).[93] Jamison et al. used this synthetic strategy as an alternative to the classical amide bond formation in (oligo)peptide synthesis without the usually applied coupling reagents and necessary separation steps. It must be noted here that this work is a rare example of using a customized quartz glass tubing (0.625 mL, i.d. = 0.762 mm) instead of an UV-transparent polymer capillary. A medium-pressure Hg lamp was applied (450 W) as a light source without filter equipment. Process development was done with nitrone **152**, which was readily prepared by condensing p-tolualdehyde with methyl hydroxylamine hydrochloride in CH$_2$Cl$_2$ and NEt$_3$ as an additional base. The nitrone was dissolved in aceto-
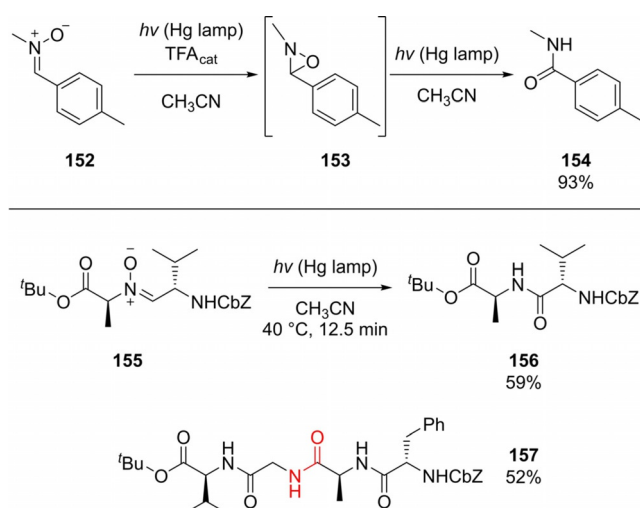
Figure 30. Top: Photolytic rearrangement of oxaziridines as the key step in the synthesis of a monocyclic lactam. Bottom: Single chiral bicyclic lactam **151** derived from bicyclic ketone **148**.

Figure 31. Top: Photochemical amide group formation via nitrone and oxaziridine rearrangement in continuous flow ($\tau_{res} = 10$ min; TFA = trifluoroacetic acid). Bottom: Functional group tolerant rearrangement of nitrones for the formation of fully protected dipeptide ʟ-Ala-ʟ-Val **156** as well as tetrapeptide ʟ-Val-Gly-ʟ-Ala-ʟ-Phe **157**.

nitrile (0.05 M) with 0.25 equivalents of TFA as the catalytic additive. Full conversion with 93% yield of the desired amide group was achieved within a residence time of $\tau_{res} = 10$ min at a rather high temperature of $T = 92\,°C$.

The optimized reaction conditions were then used as a base for the amide coupling of amino acids. L-Ala-derived hydroxylamine and L-valine-derived aldehyde were condensed to the desired nitrone **155**, which was then fed into the photoreactor (0.1 M in acetonitrile without additive). A slightly prolonged residence time of $\tau_{res} = 12.5$ min was necessary to obtain the desired dipeptide **156** in 59% yield with full conversion of the nitrone at 40 °C. For comparison, a batch reaction was performed in a quartz NMR tube (i.d. 5 mm) with an irradiation time of 10 min, yielding the oxaziridine intermediate as the major product. Other amino acids were subjected to this synthesis route as well, showing a very good tolerance to various, but necessarily full protected side chains. The sole exception is cysteine. Independent of the protecting group on the sulfur atom, decomposition of the oxaziridine takes place. Larger peptides were obtained as well, as exemplified with Val-Gly-Ala-Phe (**157**) in 52% yield. The authors also suggest the use of their coupling methodology for protein engineering by using a bis-aldehyde as linker between two proteins with reactive hydroxylamine groups readily available for nitrone formation.

3. Conclusion and Outlook

Flow photochemistry is a lively research field with numerous developments throughout the complete area of synthetic organic chemistry. The decision on the choice of topics for this review was hampered by the overwhelming number of new publications per month. Just recently, Singh et al. published a continuous-flow hydrogenation protocol for the catalyst-free photoreduction of *ortho*-methyl phenyl ketones with water as the hydrogen source.[94] Kappe et al. applied flow technology for the in situ formation of bromine, which was directly used in a subsequent step for the photochemical bromination of benzylic positions.[95] Meng et al. performed the continuous-flow enantioselective α-hydroxylation of β-dicarbonyl compounds with a cinchona-derived phase transfer organocatalyst for chirality transfer and TPP for singlet oxygen formation.[96] And finally, Koenigs et al. published their work on the photolysis of aryl diazoacetates for carbene transfer chemistry in continuous-flow equipment.[97] These examples represent just a small number of new publications, but a broad range of applications for flow photochemistry in fine chemicals synthesis. The process of knowledge transfer from simple reactions in photochemistry and photocatalysis to complex starting materials and catalyst systems is unbroken. Microreaction technology and adjunct concepts from continuous-flow chemistry provide an important background to drive photochemical reactions in a most efficient and sustainable manner. As exemplified in this review, the transfer from batch to flow resulted in multiple benefits for the photochemical process with, for example, reduction in reaction time, less waste owing to higher concentrations with increased conversion rates, easier process scale-up,

novel reaction pathways and selectivities, as well as the possibility to implement advanced online analytical tools. With these advantages named, flow photochemistry has a large overlap with the principles of Green Chemistry.[98] Associated with this trend, it has become apparent in recent years that photochemistry is connected to well-known catalysis concepts like organocatalysis and noble metal catalysis.[21] Recently, the combination of visible-light photochemistry with biocatalysis has attracted attention as well, as it allows the highly selective production of fine chemicals under very mild conditions.[99] Currently, this methodology is mainly used for the regeneration of the co-factors applied to the biocatalytic cycle, but recent developments point to new directions with photoenzymes, tandem, and concurrent photobiocatalysis.[100]

Besides this general trend for a more sustainable chemistry, the advancement of technology for flow photochemistry is ongoing as well. As mentioned before, continuous-flow equipment for photochemistry is meanwhile commercially available and allows nearly any research group to get in touch with this technology.[8] In addition, reactor concepts have also been advanced for large photochemical flow processes (e.g., the Firefly reactor with kilogram scale) or known designs like the spinning disc reactor have been adapted to photochemical applications.[101] In consequence, with such new technology at hand, academic scientists and chemical industry now have plentiful possibilities for developing new chemical syntheses and producing fine chemicals with light.

Another hot topic is the utilization of solar light for energy harvesting in general, but also as the energy source for photochemical syntheses. The current research in solar light harvesting is a consequence of the fact that fossil fuels will not last forever, disregarding their harmful impact on the climate after burning them for energy generation. National and international funding agencies have set up large research programs to investigate relevant technologies and concepts for the use of solar light. Academic and fundamental research about, for example, materials, electrodes, and membranes for light conversion and harvesting will be funded as well as the development of new photoactive systems.[102] More application-oriented research is planned in industry-driven projects supported by the European Commission for, for example, the conversion of solar light to chemical energy carriers or the use of solar light in industrial processes.[103] World-wide networks like Mission Innovation have been established to join forces to solve the most apparent challenges of a sustainable energy supply with solar fuels.[104] Finally, large-scale research initiatives have been founded, which perform research on the scientific, technological, and the societal level. This holistic approach has its focus on understanding and solving the technological and scientific challenges of the necessary paradigm change in energy supply, and the most important need to explain the facts and consequences to the everyday consumer.[105]

In summary, photochemistry and its application in continuous-flow mode has found its way into the laboratories and technical centers of universities and industries. It is one important part of the enduring change in thinking and doing chemistry with the goal of a sustainable future. Fine chemicals

in high quality are necessary for everyday needs and must be available for an acceptable price. They cannot be "decarbonized" as has been discussed and performed already in part for fossil fuels as their equivalents in the energy sector. In consequence, future research must be intensified regarding new photocatalysis concepts for visible and infrared light, immobilization of catalyst material, and waste-reduction via biomass valorization in fine chemicals synthesis. With these challenges solved, flow photochemistry will become even more aligned to the concepts of Green Chemistry for a sustainable future.

Acknowledgements

Conflict of interest

The authors declare no conflict of interest.

Keywords: continuous flow · green chemistry · intensification · photocatalysis · safety

[1] a) K. Jänisch, V. Hessel, H. Löwe, M. Baerns, *Angew. Chem. Int. Ed.* **2004**, *43*, 406–446; *Angew. Chem.* **2004**, *116*, 410–451; b) *Flow Chemistry: Fundamentals & Applications, Vol. 1–2* (Eds.: F. Darvas, V. Hessel, G. Dorman), De Gruyter, Berlin, **2014**; c) M. B. Plutschack, B. Pieber, K. Gilmore, P. H. Seeberger, *Chem. Rev.* **2017**, *117*, 11796–11893; d) I. Rossetti, M. Compagnoni, *Chem. Eng. J.* **2016**, *296*, 56–70.

[2] a) *Micro Process Engineering: A Comprehensive Textbook* (Eds.: V. Hessel, A. Renken, J. Schouten, J.-I. Yoshida), Wiley-VCH, Weinheim, **2013**; b) *Novel Process Windows: Innovative Gates to Intensified and Sustainable Chemical Process* (Eds.: V. Hessel, D. Kralisch, N. Kockmann), Wiley-VCH, Weinheim, **2015**; c) *Sustainable Flow Chemistry* (Ed.: L. Vaccaro), Wiley-VCH, Weinheim, **2017**.

[3] a) "Continuous-flow photochemistry in microstructured environment": T. H. Rehm in: *Flow Chemistry: Applications* (Eds.: F. Darvas, V. Hessel, G. Dorman), De Gruyter, Berlin, **2014**; b) K. Mizuno, Y. Nishiyama, T. Ogaki, K. Terao, H. Ikeda, K. Kakiuchi, *J. Photochem. Photobiol. C* **2016**, *29*, 107–147.

[4] a) Y. Sun, Y. Jiang, X. Sun, S. Zhang, S. Chen, *Chem. Rec.* **2019**, *19*, 1729–1752; b) S. Li, S.-C. Tan, C. Lee, E. Waffenschmidt, S. Hui, C. Tse, *IEEE Trans. Power Electr.* **2016**, *31*, 1503–1516; c) M. Kneissl, T. Kolbe, C. Chua, V. Kueller, N. Lobo, J. Stellmach, A. Knauer, H. Rodriguez, S. Einfeldt, Z. Yang, N. Johnson, M. Weyers, *Semicond. Sci. Technol.* **2011**, *26*, 014036; d) P. Xiao, J. Huang, Y. Yu, B. Liu, *Molecules* **2019**, *24*, 151–179; e) L. Quan, P. de Qrquer, R. Sabatini, E. Sargent, *Adv. Mater.* **2018**, *30*, 1801996; f) Y. Wei, Z. Cheng, J. Li, *Chem. Soc. Rev.* **2019**, *48*, 310–350; g) T. Wu, C.-W. Sher, Y. Lin, C.-F. Lee, S. Liang, Y. Lu, S.-W. Chen, W. Guo, H.-C. Kuo, Z. Chen, *Appl. Sci.* **2018**, *8*, 1557–1574; h) S. Nakamura, *Angew. Chem. Int. Ed.* **2015**, *54*, 7770–7788; *Angew. Chem.* **2015**, *127*, 7880–7899; D. Ziegenbalg, G. Kreisel, D. Weis, D. Kralisch, *Photochem. Photobiol. Sci.* **2014**, *13*, 1005–1015.

[5] a) A. Cassano, C. Martín, R. Brandi, O. Alfano, *Ind. Eng. Chem. Res.* **1995**, *34*, 2155–2201; b) T. van Gerven, G. Mul, J. Moulijn, A. Stankiewicz, *Chem. Eng. Process.* **2007**, *46*, 781–789; c) D. Ziegenbalg, B. Wriedt, G.

Kreisel, D. Kralisch, *Chem. Eng. Technol.* **2016**, *39*, 123–134; d) K. Loubière, M. Oelgemöller, T. Aillet, O. Dechy-Cabaret, L. Prat, *Chem. Eng. Process.* **2016**, *104*, 120–132; e) M. Sender, D. Ziegenbalg, *Chem. Ing. Tech.* **2017**, *89*, 1159–1173; f) M. Martín-Sómer, C. Pablos, R. van Grieken, J. Marugán, *Appl. Catal. B* **2017**, *215*, 1–7; g) B. Wriedt, D. Kowalczyk, D. Ziegenbalg, *ChemPhotoChem* **2018**, *2*, 913–921; h) R. Radjagobalou, J.-F. Blanco, O. Dechy-Carbaret, M. Oelgemöller, K. Loubiere, *Chem. Eng. Proc. Process Intensification* **2018**, *130*, 214–228; i) E. Moschetta, S. Richter, S. Wittenberger, *ChemPhotoChem* **2017**, *1*, 539–543; j) G. Glotz, O. Kappe, *React. Chem. Eng.* **2018**, *3*, 478–486; k) K. Loponov, J. Lopes, M. Barlog, E. Astrova, A. Malkov, A. Lapkin, *Org. Process Res. Dev.* **2014**, *18*, 1443–1454.

[6] L. Elliott, J. Knowles, P. Koovits, K. Maskill, M. Ralph, G. Lejeune, L. Edwards, R. Robinson, I. Clemens, B. Cox, D. Pascoe, G. Koch, M. Eberle, M. Berry, K. Booker-Milburn, *Chem. Eur. J.* **2014**, *20*, 15226–15232.

[7] N. Straathof, Y. Su, V. Hessel, T. Noël, *Nat. Protoc.* **2016**, *11*, 10–21.

[8] Some suppliers of complete systems for flow photochemistry, see: Vapourtec Ltd. (www.vapourtec.com); FutureChemistry Holding BV (www.futurechemistry.com); Creaflow (www.creaflow.be); Peschl Ultraviolet GmbH (www.peschl-ultraviolet.com); Corning Inc. (www.corning.com).

[9] For a general overview on photochemistry in continuous-flow mode, see: a) *Photochemical Processes in Continuous-Flow Reactors: From Engineering Principles to Chemical Applications* (Ed.: T. Noël), World Scientific, London, **2017**; b) Y. Su, N. Straathof, V. Hessel, T. Noël, *Chem. Eur. J.* **2014**, *20*, 10562–10589; c) J. Knowles, L. Elliott, K. Booker-Milburn, *Beilstein J. Org. Chem.* **2012**, *8*, 2025–2052; d) K. Gilmore, P. Seeberger, *Chem. Rec.* **2014**, *14*, 410–418; e) D. Cambié, C. Bottecchia, N. Straathof, V. Hessel, T. Noël, *Chem. Rev.* **2016**, *116*, 10276–10341; f) F. Politano, G. Oksdath-Mansilla, *Org. Process Res. Dev.* **2018**, *22*, 1045–1062; g) D. Heggo, S. Ookawara, *Chem. Eng. Sci.* **2017**, *169*, 67–77; h) Special Issue: Flow Photochemistry: *ChemPhotoChem* **2018**, *2*, https://onlinelibrary.wiley.com/toc/23670932/2018/2/10 (website accessed 04.03.2019).

[10] Further examples for fine chemical synthesis using flow photochemistry: a) B. Anderson, W. Bauta, W. Cantrell, *Org. Process Res. Dev.* **2012**, *16*, 967–975; b) M. Baumann, I. Baxendale, *React. Chem. Eng.* **2016**, *1*, 147–150; c) X.-Z. Fan, J.-W. Rong, H.-L. Wu, Q. Zhou, H.-P. Deng, J. Tan, C.-W. Xue, L.-Z. Wu, H.-R. Tao, J. Wu, *Angew. Chem. Int. Ed.* **2018**, *57*, 8514–8518; *Angew. Chem.* **2018**, *130*, 8650–8654; d) F. Kloss, T. Neuwirth, V. Haensch, C. Hertweck, *Angew. Chem. Int. Ed.* **2018**, *57*, 14476–14481; *Angew. Chem.* **2018**, *130*, 14684–14689; e) M. Lesieur, C. Battilocchio, R. Labes, J. Jacq, C. Genicot, S. Ley, P. Pasau, *Chem. Eur. J.* **2019**, *25*, 1203–1207; f) M. Czarnecki, P. Wessig, *Org. Process Res. Dev.* **2018**, *22*, 1823–1827; g) Z. Hamami, L. Vanoye, P. Fongarland, C. de Bellefon, A. Favre-Réguillon, *ChemPhotoChem* **2019**, *3*, 122–128; h) D. Cambié, T. Noël, *Top. Curr. Chem.* **2018**, *376*, 45.

[11] Further examples for continuous-flow synthesis of materials using photochemistry: a) T. Junkers, B. Wenn, *React. Chem. Eng.* **2016**, *1*, 60–64; b) H. du Toit, T. Macdonald, H. Huang, I. Parkin, A. Gavriilidis, *RSC Adv.* **2017**, *7*, 9632–9638; c) J. Vrijsen, C. Medeiros, J. Gruber, T. Junkers, *Polym. Chem.* **2019**, *10*, 1591–1598; d) A. Melker, B. Fors, C. Hawker, J. Poelma, *J. Polym. Sci. Pol. Chem.* **2015**, *53*, 2693–2698.

[12] Further examples of flow photochemistry using specialized equipment: a) E. Bremus-Köbberling, A. Gillner, F. Avemaria, C. Réthore, S. Bräse, *Beilstein J. Org. Chem.* **2012**, *8*, 1213–1218; b) C. Shen, Y. Wang, J. Hu, G. Luo, *Chem. Eng. J.* **2015**, *277*, 48–55; c) M. Sellaro, M. Bellardite, A. Brunetti, E. Fontananova, L. Palmisano, E. Drioli, G. Barbieri, *RSC Adv.* **2016**, *6*, 67418–67427; d) B. da Costa Filho, A. Araujo, B. Silva, R. Boaventura, M. Dias, J. Lopes, V. Vilar, *Chem. Eng. J.* **2017**, *310*, 331–341; e) Y. Pihosh, J. Uemera, I. Turkevych, K. Mawatari, Y. Kazoe, A. Smirnova, T. Kitamori, *Angew. Chem. Int. Ed.* **2017**, *56*, 8130–8133; *Angew. Chem.* **2017**, *129*, 8242–8245; f) A. Kouridaki, K. Huvaere, *React. Chem. Eng.* **2017**, *2*, 590–597; g) J. Williams, M. Nakano, R. Gérady, J. Rincón, Ó. de Frutos, C. Mateos, J.-C. Monbaliu, O. Kappe, *Org. Process Res. Dev.* **2019**, *23*, 78–87; h) L. Lin, K. Xie, M. Beaucamp, N. Job, M. Penhoat, *ChemPhotoChem* **2019**, *3*, 198–203; i) J. Schachtner, A. von Wangelin, *Beilstein J. Org. Chem.* **2016**, *12*, 1798–1811.

[13] a) *Chemical Photocatalysis* (Ed.: B. König), DeGruyter, Berlin, **2013**; b) H. Kisch, *Semiconductor Photocatalysis: Principles and Applications*, Wiley-VCH, Weinheim, **2015**; c) *Natural and Artificial Photosynthesis: Solar*

Chemistry–A European Journal

Review
doi.org/10.1002/chem.202000381

Chemistry Europe
European Chemical
Societies Publishing

Power as an Energy Source (Ed.: R. Razeghifard), Wiley, New Jersey, **2013**; d) *Visible Light Photocatalysis in Organic Chemistry* (Eds.: C. Stephenson, T. Yoon, D. MacMillan), Wiley-VCH, Weinheim, **2018**; e) C. Prier, D. Rankic, D. MacMillan, *Chem. Rev.* **2013**, *113*, 5322–5364; f) D. Hari, B. König, *Chem. Commun.* **2014**, *50*, 6688–6699; g) N. Romero, D. Nicewicz, *Chem. Rev.* **2016**, *116*, 10075–10166; h) M. Kärkäs, J. Porco, C. Stephenson, *Chem. Rev.* **2016**, *116*, 9683–9747; i) V. Ramamurthy, J. Sivaguru, *Chem. Rev.* **2016**, *116*, 9914–9993; j) L. Marzo, S. Pagire, O. Reiser, B. König, *Angew. Chem. Int. Ed.* **2018**, *57*, 10034–10072; *Angew. Chem.* **2018**, *130*, 10188–10228; k) D. Ravelli, M. Fagnoni, A. Albini, *Chem. Soc. Rev.* **2013**, *42*, 97–113; l) R. Brimioulle, D. Lenhart, M. Maturi, T. Bach, *Angew. Chem. Int. Ed.* **2015**, *54*, 3872–3890; *Angew. Chem.* **2015**, *127*, 3944–3963; m) J. Beatty, C. Stephenson, *Acc. Chem. Res.* **2015**, *48*, 1474–1484; n) D. Staveness, I. Bosque, C. Stephenson, *Acc. Chem. Res.* **2016**, *49*, 2295–2306; o) J.-R. Chen, X.-Q. Hu, L.-Q. Lu, W.-J. Xiao, *Acc. Chem. Res.* **2016**, *49*, 1911–1923; p) O. Reiser, *Acc. Chem. Res.* **2016**, *49*, 1990–1996; q) Y.-Q. Zou, F. Hörmann, T. Bach, *Chem. Soc. Rev.* **2018**, *47*, 278–290; r) T. Yoon, M. Ischay, J. Du, *Nat. Chem.* **2010**, *2*, 527–532.

[14] a) O. Wenger, *Chem. Eur. J.* **2019**, *25*, 6043–6052; b) S. Otto, A. Nauth, E. Ermilov, N. Scholz, A. Friedrich, U. Resch-Geger, S. Lochbrunner, T. Opatz, K. Heinze, *ChemPhotoChem* **2017**, *1*, 344–349; c) S. Treiling, C. Wang, C. Förster, F. Reichenauer, J. Kalmbach, P. Boden, J. Harris, L. Carrella, E. Rentschler, U. Resch-Genger, C. Reber, M. Seitz, M. Gerhards, K. Heinze, *Angew. Chem. Int. Ed.* **2019**, *58*, 18075–18085; *Angew. Chem.* **2019**, *131*, 18243–18253.

[15] a) D. Ravelli, M. Fagnoni, *ChemCatChem* **2012**, *4*, 169–171; b) J. Barona-Castaño, C. Carmona-Vargas, T. Brockson, K. de Oliveira, *Molecules* **2016**, *21*, 310–337; G. de Gonzalo, M. Fraaije, *ChemCatChem* **2013**, *5*, 403–415.

[16] a) L. Zeng, T. Liu, C. He, D. Shi, F. Zhang, C. Duan, *J. Am. Chem. Soc.* **2016**, *138*, 3958–3961; b) H.-X. Gong, Z. Cao, M.-H. Li, S.-H. Liao, M.-J. Lin, *Org. Chem. Front.* **2018**, *5*, 2296–2302; c) X. Feng, P. Liao, J. Jiang, J. Shi, Z. Ke, J. Zhang, *ChemPhotoChem* **2019**, *3*, 1014–1019.

[17] a) J. Ge, Y. Zhang, S.-J. Park, *Materials* **2019**, *12*, 1916–1942; b) X. Wang, K. Maeda, A. Thomas, K. Takanabe, G. Xin, J. Carlsson, K. Domen, M. Antonietti, *Nat. Mater.* **2009**, *8*, 76–80; c) F. Su, S. Mathew, G. Lipner, X. Fu, M. Antonietti, S. Blechert, X. Wang, *J. Am. Chem. Soc.* **2010**, *132*, 16299–16301; d) L. Möhlmann, M. Baar, J. Rieß, M. Antonietti, X. Wang, S. Blechert, *Adv. Synth. Catal.* **2012**, *354*, 1909–1913; e) B. Pieber, J. Malik, C. Cavedon, S. Gisbertz, A. Savateev, D. Cruz, T. Heil, G. Zhang, P. Seeberger, *Angew. Chem. Int. Ed.* **2019**, *58*, 9575–9580; *Angew. Chem.* **2019**, *131*, 9676–9681.

[18] a) G. Duret, R. Quinlan, P. Bisseret, N. Blanchard, *Chem. Sci.* **2015**, *6*, 5366–5382; b) D. DiRocco, *Electrochemical Series of Photocatalysts and Common Organic Compounds* **2014**, https://vdocuments.site/photocatalysts-chart-dirocco.html (website accessed on 18.12.2019).

[19] a) P. Riente, T. Noël, *Catal. Sci. Technol.* **2019**, *9*, 5186–5232; b) H. Tan, F. Abdi, Y. Ng, *Chem. Soc. Rev.* **2019**, *48*, 1255–1271.

[20] a) R. Asahi, T. Morikawa, T. Ohwaki, K. Aoki, Y. Taga, *Science* **2001**, *293*, 269–271; b) J. Varley, A. Janotti, C. Van de Walle, *Adv. Mater.* **2011**, *23*, 2343–2347; c) C.-H. Lee, E. Galoppini, *J. Org. Chem.* **2010**, *75*, 3692–3704; d) A. Nauth, E. Schechtel, R. Dören, W. Tremel, T. Opatz, *J. Am. Chem. Soc.* **2018**, *140*, 14169–14177; e) A. Carrillo, A. Elhage, L. Marin, A. Lanterna, *Chem. Eur. J.* **2019**, *25*, 14928–14934.

[21] a) J. Tellis, C. Kelly, D. Primer, M. Jouffroy, N. Patel, G. Molander, *Acc. Chem. Res.* **2016**, *49*, 1429–1439; b) X. Lang, J. Zhao, X. Chen, *Chem. Soc. Rev.* **2016**, *45*, 3026–3028; c) K. Skubi, T. Blum, T. Yoon, *Chem. Rev.* **2016**, *116*, 10035–10074; d) J. Milligan, J. Phelan, S. Badir, G. Molander, *Angew. Chem. Int. Ed.* **2019**, *58*, 6152–6163; *Angew. Chem.* **2019**, *131*, 6212–6224; e) I. Perry, T. Brewer, P. Sarver, D. Schultze, D. DiRocco, D. MacMillan, *Nature* **2018**, *560*, 70–75; –f) Q.-Y. Meng, S. Wang, B. König, *Angew. Chem. Int. Ed.* **2017**, *56*, 13426–13430; *Angew. Chem.* **2017**, *129*, 13611–13615; g) M. Hopkinson, B. Sahoo, J.-L. Li, F. Glorius, *Chem. Eur. J.* **2014**, *20*, 3874–3886; h) D. Fabry, M. Rueping, *Acc. Chem. Res.* **2016**, *49*, 1969–1979; i) M. Silvi, P. Melchiorre, *Nature* **2018**, *554*, 41–49; j) B. Mühldorf, R. Wolf, *Angew. Chem. Int. Ed.* **2016**, *55*, 427–430; *Angew. Chem.* **2016**, *128*, 437–441.

[22] a) E. Arceo, I. Jurberg, A. Álvarez-Fernández, P. Melchiorre, *Nat. Chem.* **2013**, *5*, 750–756; b) M. Pirnot, D. Rankic, D. Martin, D. MacMillan, *Science* **2013**, *339*, 1593–1596; c) H. Hoa, X. Shen, C. Wang, L. Zhang, P.

Röse, L.-A. Chen, K. Harms, M. Marsch, G. Hilt, E. Meggers, *Nature* **2014**, *515*, 100–103; d) J. Metternich, R. Gilmour, *J. Am. Chem. Soc.* **2016**, *138*, 1040–1045; e) J. McManus, D. Nicewicz, *J. Am. Chem. Soc.* **2017**, *139*, 2880–2883; f) L. Wozniak, G. Magagnano, P. Melchiorre, *Angew. Chem. Int. Ed.* **2018**, *57*, 1068–1072; *Angew. Chem.* **2018**, *130*, 1080–1084; g) I. Ghosh, R. Shaikh, B. König, *Angew. Chem. Int. Ed.* **2017**, *56*, 8544–8549; *Angew. Chem.* **2017**, *129*, 8664–8669; h) G. Goti, B. Bieszczad, A. Vega-Peñaloza, P. Melchiorre, *Angew. Chem. Int. Ed.* **2019**, *58*, 1213–1217; *Angew. Chem.* **2019**, *131*, 1226–1230; i) T. Chisholm, D. Clayton, L. Dowman, J. Sayers, R. Payne, *J. Am. Chem. Soc.* **2018**, *140*, 9020–9024; j) C. Kerzig, X. Guo, O. Wenger, *J. Am. Chem. Soc.* **2019**, *141*, 2122–2127; k) N. Ichiishi, J. Caldwell, M. Lin, W. Zhong, X. Zhu, E. Streckfuss, H.-Y. Kim, C. Parish, S. Krska, *Chem. Sci.* **2018**, *9*, 4168–4175; l) J. Li, D. Zhu, L. Lv, C.-J. Li, *Chem. Sci.* **2018**, *9*, 5781–5786; m) K. Singh, S. Staig, J. Weaver, *J. Am. Chem. Soc.* **2014**, *136*, 5275–5278; n) B. Liu, C.-H. Lim, G. Miyake, *J. Am. Chem. Soc.* **2017**, *139*, 13616–13619; o) D. Rombach, H.-A. Wagenknecht, *ChemCatChem* **2018**, *10*, 2955–2961; p) I. Jurberg, H. Davies, *Chem. Sci.* **2018**, *9*, 5112–5118.

[23] a) I. Ghosh, T. Ghosh, J. Bardagi, B. König, *Science* **2014**, *346*, 725–728; b) I. Ghosh, B. König, *Angew. Chem. Int. Ed.* **2016**, *55*, 7676–7679; *Angew. Chem.* **2016**, *128*, 7806–7810; c) J. Haimerl, I. Ghosh, B. König, J. Vogelsang, J. Lupton, *Chem. Sci.* **2019**, *10*, 681–687.

[24] a) M. Majek, A. von Wangelin, *Acc. Chem. Res.* **2016**, *49*, 2316–2327; b) S. Protti, D. Ravelli, M. Fagnoni, *Photochem. Photobiol. Sci.* **2019**, *18*, 2094–2101; c) J.-R. Chen, D.-M. Yan, Q. Wie, W.-J. Xiao, *ChemPhotoChem* **2017**, *1*, 148–158; d) V. Balzani, G. Bergamini, P. Ceroni, *Angew. Chem. Int. Ed.* **2015**, *54*, 11320–11337; *Angew. Chem.* **2015**, *127*, 11474–11492.

[25] P. Klán, J. Wirz, *Photochemistry of Organic Compounds: From Concepts to Practice*, Wiley, Chichester, **2009**.

[26] Displayed data was obtained by analyzing the Web of Science Core Collection (Science Citation Index Expanded) from 1970 to 2019 for the topics "photocatalysis" AND "flow" (website accessed 20.01.2020).

[27] a) A. Ghogare, A. Geer, *Chem. Rev.* **2016**, *116*, 9994–10034; b) A. Burgard, T. Gieshoff, A. Peschl, D. Hörstermann, C. Keleschovsky, R. Villa, S. Michelis, M. Feth, *Chem. Eng. J.* **2016**, *294*, 83–96.

[28] a) F. Lévesque, P. Seeberger, *Angew. Chem. Int. Ed.* **2012**, *51*, 1706–1709; *Angew. Chem.* **2012**, *124*, 1738–1741; b) D. Kopetzki, F. Lévesque, P. Seeberger, *Chem. Eur. J.* **2013**, *19*, 5450–5456.

[29] S. Triemer, K. Gilmore, G. Vu, P. Seeberger, A. Seidel-Morgenstern, *Angew. Chem. Int. Ed.* **2018**, *57*, 5525–5528; *Angew. Chem.* **2018**, *130*, 5623–5626.

[30] B. Pieber, T. Glasnov, O. Kappe, *Chem. Eur. J.* **2015**, *21*, 4368–4376.

[31] D. Cambié, J. Dobbelaar, P. Riente, J. Vanderspikken, C. Shen, P. Seeberger, K. Gilmore, M. Debije, T. Noël, *Angew. Chem. Int. Ed.* **2019**, *58*, 14374–14378; *Angew. Chem.* **2019**, *131*, 14512–14516.

[32] Z. Amara, J. Bellamy, R. Horvath, S. Miller, A. Beeby, A. Burgard, K. Rossen, M. Poliakoff, M. George, *Nat. Chem.* **2015**, *7*, 489–495.

[33] L.-K. Sy, G. Brown, *Tetrahedron* **2002**, *58*, 897–908.

[34] a) F. Fleming, *Nat. Prod. Rep.* **1999**, *16*, 597–606; b) F. Fleming, L. Yao, P. Ravikumar, L. Funk, B. Shook, *J. Med. Chem.* **2010**, *53*, 7902–7917; c) N. Otto, T. Opatz, *Chem. Eur. J.* **2014**, *20*, 13064–13077.

[35] D. Ushakov, K. Gilmore, D. Kopetzki, T. McQuade, P. Seeberger, *Angew. Chem. Int. Ed.* **2014**, *53*, 557–561; *Angew. Chem.* **2014**, *126*, 568–572.

[36] S. Vukelić, D. Ushakov, K. Gilmore, B. Koksch, P. Seeberger, *Eur. J. Org. Chem.* **2015**, 3036–3019.

[37] A. Nauth, A. Lipp, B. Lipp, T. Opatz, *Eur. J. Org. Chem.* **2017**, 2099–2113.

[38] L. Capaldo, D. Ravelli, *Eur. J. Org. Chem.* **2017**, 2056–2071.

[39] D. Ravelli, S. Protti, M. Fagnoni, *Acc. Chem. Res.* **2016**, *49*, 2232–2242.

[40] M. Fagnoni, F. Bonassi, A. Palmieri, S. Protti, D. Ravelli, R. Ballini, *Adv. Synth. Catal.* **2014**, *356*, 753–758.

[41] D. Schultz, F. Lévesque, D. DiRocco, M. Reibarkh, Y. Ji, L. Joyce, J. Dropinski, H. Sheng, B. Sherry, I. Davies, *Angew. Chem. Int. Ed.* **2017**, *56*, 15274–15278; *Angew. Chem.* **2017**, *129*, 15476–15480.

[42] G. Laudadio, S. Govaerts, Y. Wang, D. Ravelli, H. Koolman, M. Fagnoni, S. Djuric, T. Noël, *Angew. Chem. Int. Ed.* **2018**, *57*, 4078–4082; *Angew. Chem.* **2018**, *130*, 4142–4146.

[43] A. Hu, J.-J. Guo, H. Pan, Z. Zuo, *Science* **2018**, *361*, 668–672.

[44] B. Zhang, A. Studer, *Chem. Soc. Rev.* **2015**, *44*, 3505–3521.

[45] Y. Fang, G. Tranmer, *Med. Chem. Commun.* **2016**, *7*, 720–724.

[46] X. Liu, J.-F. Xu, Z. Wang, X. Zhang, *Polym. Chem.* **2016**, *7*, 2333–2336.

[47] a) C. Clémenson, E. Jounanot, A. Merino-Trigo, C. Rubin-Carrez, E. Deutsch, *Invest. New Drugs* **2013**, *31*, 273–284; b) J.-Y. Blay, Z. Pápai, A. Tolcher, A. Italiano, D. Cupissol, A. López-pousa, S. Chawla, E. Bompas, N. Babovic, N. Penel, N. Isambert, A. Staddon, E. Saâda-Bouzid, A. Santoro, F. Franke, P. Cohen, S. Le-Guennec, G. Demetri, *Lancet Oncol.* **2015**, *16*, 531–540.

[48] D. Fabry, M. Ronge, M. Rueping, *Chem. Eur. J.* **2015**, *21*, 5350–5354.

[49] D. Rackl, P. Kreitmeier, O. Reiser, *Green Chem.* **2016**, *18*, 214–219.

[50] M. Royzen, G. Yap, J. Fox, *J. Am. Chem. Soc.* **2008**, *130*, 3760–3761.

[51] E. Billaud, E. Shahbazali, M. Ahamed, F. Cleeren, T. Noël, M. Koole, A. Verbruggen, V. Hessel, G. Bormans, *Chem. Sci.* **2017**, *8*, 1251–1258.

[52] D. Blanco-Ania, L. Maartense, F. Rutjes, *ChemPhotoChem* **2018**, *2*, 898–905.

[53] a) S. Purser, P. Moore, S. Swallow, V. Gouverneur, *Chem. Soc. Rev.* **2008**, *37*, 320–330; b) P. Jeschke, *ChemBioChem* **2004**, *5*, 570–589.

[54] Fluorination Reagents for Fluorination, Difluoromethylation, and Trifluoromethylation Chemistry: https://www.sigmaaldrich.com/chemistry/chemistry-products.html?TablePage=110962212 (website accessed 13.04.2018).

[55] M. Rueda-Becerril, O. Mahé, M. Drouin, M. Majewski, J. West, M. Wolf, G. Sammis, J.-F. Paquin, *J. Am. Chem. Soc.* **2014**, *136*, 2637–2641.

[56] D. Cantillo, O. de Frutos, J. Rincón, C. Mateos, O. Kappe, *J. Org. Chem.* **2014**, *79*, 8486–8490.

[57] P. Champagne, J. Desroches, J.-D. Hamel, M. Vandamme, J.-F. Paquin, *Chem. Rev.* **2015**, *115*, 9073–9174.

[58] A. McTeague, T. Jamison, *Angew. Chem. Int. Ed.* **2016**, *55*, 15072–15075; *Angew. Chem.* **2016**, *128*, 15296–15299.

[59] Intergovernmental Panel on Climate Change: http://www.ipcc.ch/publications_and_data/ar4/wg1/en/ch2s2-10-2.html (website accessed 04.05.2018).

[60] N. Straathof, H. Gemoets, X. Wang, J. Schouten, V. Hessel, T. Noël, *ChemSusChem* **2014**, *7*, 1612–1617.

[61] N. Straathof, B. Tegelbeckers, V. Hessel, X. Wang, T. Noël, *Chem. Sci.* **2014**, *5*, 4768–4773.

[62] X.-J. Wei, T. Noël, *J. Org. Chem.* **2018**, *83*, 11377–11384.

[63] N. Straathof, S. Cramer, V. Hessel, T. Noël, *Angew. Chem. Int. Ed.* **2016**, *55*, 15549–15553; *Angew. Chem.* **2016**, *128*, 15778–15782.

[64] A. Singh, C. Fennell, J. Weaver, *Chem. Sci.* **2016**, *7*, 6796–6802.

[65] J. Beatty, J. Douglas, K. Cole, C. Stephenson, *Nat. Commun.* **2015**, *6*, 7919–7925.

[66] J. Beatty, J. Douglas, R. McAtee, K. Cole, C. Stephenson, *Chem* **2016**, *1*, 456–472.

[67] a) F. Mo, G. Dong, Y. Zhang, J. Wang, *Org. Biomol. Chem.* **2013**, *11*, 1582–1593; b) F.-X. Felpin, S. Sengupta, *Chem. Soc. Rev.* **2019**, *48*, 1150–1193.

[68] D. Hari, B. König, *Angew. Chem. Int. Ed.* **2013**, *52*, 4734–4743; *Angew. Chem.* **2013**, *125*, 4832–4842.

[69] Y.-F. Liang, R. Steinbock, L. Yang, L. Ackermann, *Angew. Chem. Int. Ed.* **2018**, *57*, 10625–10629; *Angew. Chem.* **2018**, *130*, 10785–10789.

[70] C. Bottecchia, M. Rubens, S. Gunnoo, V. Hessel, A. Madder, T. Noël, *Angew. Chem. Int. Ed.* **2017**, *56*, 12702–12707; *Angew. Chem.* **2017**, *129*, 12876–12881.

[71] X. Wang, G. Cuny, T. Noël, *Angew. Chem. Int. Ed.* **2013**, *52*, 7860–7864; *Angew. Chem.* **2013**, *125*, 8014–8018.

[72] D. Cantillo, C. Mateos, J. Rincon, O. de Frutos, O. Kappe, *Chem. Eur. J.* **2015**, *21*, 12894–12898.

[73] H. Yang, B. Martin, B. Schenkel, *Org. Process Res. Dev.* **2018**, *22*, 446–456.

[74] A. Greb, J.-S. Poh, S. Greed, C. Battilocchio, P. Pasau, D. Blakemore, S. Ley, *Angew. Chem. Int. Ed.* **2017**, *56*, 16602–16605; *Angew. Chem.* **2017**, *129*, 16829–16832.

[75] M. Majchrazk, M. Bekhazi, I. Tse-Sheepy, J. Warkentin, *J. Org. Chem.* **1989**, *54*, 1842–1845.

[76] I. Abdiaj, A. Fontana, M. Gomez, A. de la Hoz, J. Alcázar, *Angew. Chem. Int. Ed.* **2018**, *57*, 8473–8477; *Angew. Chem.* **2018**, *130*, 8609–8613.

[77] M. Berton, L. Huck, J. Alcázar, *Nat. Protoc.* **2018**, *13*, 324–334.

[78] I. Abdiaj, C. Horn, J. Alcázar, *J. Org. Chem.* **2019**, *84*, 4748–4753.

[79] X.-J. Wei, I. Abdiaj, C. Sambiagio, C. Li, E. Zysman-Colman, J. Alcázar, T. Noël, *Angew. Chem. Int. Ed.* **2019**, *58*, 13030–13034; *Angew. Chem.* **2019**, *131*, 13164–13168.

[80] *Carbon Dioxide as Chemical Feedstock* (Ed.: M. Aresta), Wiley-VCH, Weinheim, **2010**, pp. 1–13.

[81] H. Seo, M. Katcher, T. Jamison, *Nat. Chem.* **2017**, *9*, 453–456.

[82] S. Matsuoka, T. Kohzuki, C. Pac, A. Ishida, S. Takamuku, M. Kusaba, N. Nakashima, S. Yanagida, *J. Phys. Chem.* **1992**, *96*, 4437–4442.

[83] H. Seo, A. Liu, T. Jamison, *J. Am. Chem. Soc.* **2017**, *139*, 13969–13972.

[84] a) L. Xu, S. Zhang, P. Li, *Chem. Soc. Rev.* **2015**, *44*, 8848–8942; b) J. Fyfe, A. Watson, *Chem* **2017**, *3*, 31–55.

[85] K. Chen, S. Zhang, P. He, P. Li, *Chem. Sci.* **2016**, *7*, 3676–3680.

[86] K. Chen, M. Cheung, Z. Lin, P. Li, *Org. Chem. Front.* **2016**, *3*, 875–879.

[87] F. Beuerle, B. Gole, *Angew. Chem. Int. Ed.* **2018**, *57*, 4850–4878; *Angew. Chem.* **2018**, *130*, 4942–4972.

[88] *Boronic Acids* (Ed.: D. Hall), Wiley-VCH, Weinheim, **2011**.

[89] a) A. Mfuh, V. Nguyen, B. Chhetri, J. Burch, J. Doyle, V. Nesterov, H. Arman, O. Larionov, *J. Am. Chem. Soc.* **2016**, *138*, 8404–8411; b) A. Mfuh, B. Schneider, W. Cruces, O. Larionov, *Nat. Protoc.* **2017**, *12*, 604–610.

[90] a) T. Bach, J. Hehn, *Angew. Chem. Int. Ed.* **2011**, *50*, 1000–1045; *Angew. Chem.* **2011**, *123*, 1032–1077; b) X.-M. Zhang, Y.-Q. Tu, F.-M. Zhang, Z.-H. Chen, S.-H. Wang, *Chem. Soc. Rev.* **2017**, *46*, 2272–2305; c) Z.-M. Chen, X.-M. Zhang, Y.-Q. Tu, *Chem. Soc. Rev.* **2015**, *44*, 5220–5245.

[91] a) A. Lattes, E. Oliveros, M. Rivière, C. Belzecki, D. Mostowicz, W. Abramskj, C. Piccinni-Leopardi, G. Germain, M. van Meerssche, *J. Am. Chem. Soc.* **1982**, *104*, 3929–3934; b) M. Wolfe, D. Dutta, J. Aubé, *J. Org. Chem.* **1997**, *62*, 654–663; c) Y. Zeng, B. Smith, J. Hershberger, J. Aubé, *J. Org. Chem.* **2003**, *68*, 8065–8067.

[92] J. Cochran, N. Waal, *Org. Process Res. Dev.* **2016**, *20*, 1533–1539.

[93] Y. Zhang, M. Blackman, A. Leduc, T. Jamison, *Angew. Chem. Int. Ed.* **2013**, *52*, 4251–4255; *Angew. Chem.* **2013**, *125*, 4345–4349.

[94] D. Aand, B. Mahajan, S. Pabbaraja, A. Singh, *React. Chem. Eng.* **2019**, *4*, 812–817.

[95] A. Steiner, J. Williams, O. de Frutos, J. Rincón, C. Mateos, O. Kappe, *Green Chem.* **2020**, *22*, 448–454.

[96] a) X.-F. Tang, J.-N. Zhao, Y.-F. Wu, S.-H. Feng, F. Yang, Z.-Y. Yu, Q.-W. Meng, *Adv. Synth. Catal.* **2019**, *361*, 5245–5252; b) X.-F. Tang, J.-N. Zhao, Y.-F. Wu, Z.-H. Zheng, S.-H. Feng, Z.-Y. Yu, G.-Z. Liu, Q.-W. Meng, *Org. Biomol. Chem.* **2019**, *17*, 7938–7942.

[97] C. Empel, R. Koenigs, *J. Flow Chem.* **2020**, *10*, 157–160.

[98] a) P. Anatas, J. Warner: *Green Chemistry: Theory and Practice*, Oxford University Press, Oxford, **1998**; b) H. C. Erythropel, J. B. Zimmerman, T. M. deWinter, L. Petitjean, F. Melnikov, C. H. Lam, A. W. Lounsbury, K. E. Mellor, N. Z. Jankovica, Q. Tu, L. N. Pincus, M. M. Falinski, W. Shi, P. Coish, D. L. Plata, P. T. Anastas, *Green Chem.* **2018**, *20*, 1929–1961.

[99] a) C. Seel, A. Králik, M. Hacker, A. Frank, B. König, T. Gulder, *ChemCatChem* **2018**, *10*, 3960–3963; b) C. Seel, T. Gulder, *ChemBioChem* **2019**, *20*, 1871–1897.

[100] a) D. Sorigué, B. Légeret, S. Cuiné, S. Blangy, S. Moulin, E. Billon, P. Richaud, S. Brugière, Y. Couté, D. Nurizzo, P. Müller, K. Brettel, D. Pignol, P. Arnoux, Y. Li-Beisson, G. Peltier, F. Beisson, *Science* **2017**, *357*, 903–907; b) C. Denard, H. Huang, M. Bartlett, L. Lu, Y. Tan, H. Zhao, J. Hartwig, *Angew. Chem. Int. Ed.* **2014**, *53*, 465–469; *Angew. Chem.* **2014**, *126*, 475–479; c) V. Köhler, N. Turner, *Chem. Commun.* **2015**, *51*, 450–464.

[101] a) T. H. Rehm, *ChemPhotoChem* **2020**, *4*, 235–254; b) L. Elliott, M. Berry, B. Haji, D. Klauber, J. Leonard, K. Booker-Milburn, *Org. Process Res. Dev.* **2016**, *20*, 1806–1811; c) A. Chaudhuri, K. Kuijpers, R. Hendrix, J. Hacking, P. Shivaprasad, E. Emanuelsson, T. Noël, j. van der Schaaf, *ChemRxiv* **2020**, DOI: https://doi.org/10.26434/chemrxiv.11560224.v1.

[102] International Call "Solar-Driven Chemistry 2019/2020" of the German Research Foundation, http://www.dfg.de/en/research_funding/announcements_proposals/2018/info_wissenschaft_18_94/index.html (website accessed 04.03.2019).

[103] EU Horizon2020 Calls "Converting Sunlight to Storable Chemical Energy (LC-SC3-RES-29-2019)" and "Solar Energy in Industrial Processes (LC-SC3-RES-7-2019)", http://ec.europa.eu/research/participants/data/ref/h2020/wp/2018-2020/main/h2020-wp1820-energy_en.pdf (website accessed 04.03.2019).

[104] Website of Mission Innovation with Innovation Challenge 5: Converting Sunlight, http://mission-innovation.net/our-work/innovation-challenges/converting-sunlight/ (website accessed 21.01.2020).

[105] Coordinating Support Actions to Large-Scale Research Initiatives of the European Union: (a) SunRise, https://www.sunriseaction.com; (b) Energy-X, https://www.energy-x.eu; (websites accessed 04.03.2019).